

Virginia Commonwealth University
VCU Scholars Compass

Theses and Dissertations | Graduate School

2017

Hydrogen Sulfide Regulation of Kir Channels

Junghoon Ha
Virginia Commonwealth University

Follow this and additional works at: https://scholarscompass.vcu.edu/etd

 Part of the Cellular and Molecular Physiology Commons, Medicine and Health Sciences Commons, and the Molecular and Cellular Neuroscience Commons

© The Author

Downloaded from
https://scholarscompass.vcu.edu/etd/5204

This Dissertation is brought to you for free and open access by the Graduate School at VCU Scholars Compass. It has been accepted for inclusion in Theses and Dissertations by an authorized administrator of VCU Scholars Compass. For more information, please contact libcompass@vcu.edu.

Hydrogen Sulfide Regulation of Kir Channels

A dissertation submitted in partial fulfillment of the requirements for the degree of Doctor of Philosophy at Virginia Commonwealth University

by

Junghoon Ha

M.S. Virginia Commonwealth University, VA, 2009

B.S. University of Virginia, Charlottesville, VA, 2004

Director: Diomedes E. Logothetis
Former John D. Bower Chair, Department of Physiology and Biophysics

Virginia Commonwealth University
Richmond, Virginia
April 2017

Acknowledgement

First and foremost, I would like to thank my thesis mentor, Dr. Diomedes Logothetis. Without his guidance and leadership, I would not have been so eager to pursue a career in becoming a physician-scientist. He has been absolutely supportive in the face of any hardships I've encountered in the past year, never ceasing to amaze me with his patience and resourcefulness. I would also like to extend my thanks to my committee members, especially Dr. Clive Baumgarten, who has been supportive throughout this process. In particular, Dr. Baumgarten has imparted me with an invaluable general overview of ion channels and electrophysiology, and this has undoubtedly enhanced my graduate experience. I'm very grateful to the late Dr. Louis De Felice for the many meetings in which he distilled complex ideas down to a few scribbles on a piece of paper and always challenging me to approach how to think of things from a different angle. I'm thankful to Dr. Hamid Akbarali whose instructions previously have shaped my understanding of ion channels. I want to thank Dr. Dana Selley for agreeing to be on this committee, and being an enthusiastic advocate despite my thesis project taking major turns away from the topics he holds most dear. And I'd like to thank Dr. Fadi Salloum for taking responsibility as my advisor of records and for his invaluable advice to bolster the quality of my thesis.

I am especially thankful to Dr. Gordon Archer for his counsel and the motivation he provided as he accepted me into the MD-PhD program. I'd be remiss if I did not mention how much I have been shaped and influenced by his steadfast standards for excellence. And I am forever grateful to Dr. Susan DiGiovanni who provided not just guidance but empathy to motivate me in my tough time during the second year in the M.D. program. I owe much to her

understanding and faith in my abilities to return to form and resume my studies. My gratitude extends to my previous mentors, Dr. Kevin Pfister and Dr. Anthony Spano who have greatly shaped my scientific thinking in the years that I was an undergraduate student and lab technician prior to my enrollment in VCU's graduate program.

I would also like to thank my colleagues and good friends, Frank Chen, Rahul Mahajan, and Vasileios Petrou for providing me with tremendous support and enabling me to think critically about my experiments. They've provided me with moral support through my personal hurdles, and have challenged my thinking and kept filling me with ideas even during the couple months when the poor oocyte health stymied my research efforts. I'm indebted to Dr. Yu Xu, who has aided in my thesis work with her computational work, as well as Dr. Takeharu Kawano for his molecular biology expertise. In addition, I'd like to acknowledge Tyler Hendon for his work on the TAG-switch assay, which corroborated my experimental results. Also, without Guoqing Xiang, Amr Ellaithy, and Sung Park keeping me company at my hours in the lab with their encouragement, I am certain my laboratory (as well as personal life) would not have sailed as smoothly. I'd also like to thank Jason Younkin for his advice on this thesis as well as his many contributions to ensure the laboratory is in optimum working order. I want to thank all of the other laboratory members of the Logothetis lab, especially Heikki Vaananen who was always available to provide me with technical support and counsel I needed to allow me to focus on the research instead of troubleshooting the equipment and methods.

My life outside of science could not have been as enriched without Jennifer Cole, who has been steadfastly caring and compassionate towards me especially during the most unpredictable phases of my life. She has been nothing but encouraging in my attainment of my

ambitions as a physician-researcher as well as this thesis work. My sincere thanks also go towards Nathan Gardner, Pascal Vicaire, Christopher Nelson, and David Del Vecchio, who despite being separated from me by geography have kept in touch with me on a frequent basis, always sensitive to my general well-being.

Lastly, and most importantly, I would like to thank my parents, Jonghye and Sangdo Ha, my brother, Jayhoon Ha, and my grandparents, Youngbae and Jungho Kim. These are the people who've colored my perspective of the world as well as my personal life. I would also like to acknowledge my aunts, Jongshin and Jongshil Kim who've treated me as if I were their very own son ever since the earliest memories I can conjure up of my childhood. Throughout the small steps I've taken in life, they've shown me it is okay to be human and fall occasionally. Without their unconditional love, I would not be where I am today.

Table of Contents

Page

Acknowledgements....ii

List of Figures and Tables....vii

List of Abbreviations....ix

Abstract....xii

Chapter 1. Background

1.1 Hydrogen Sulfide, Kir Channels, and PIP_2....1

1.2. Overview of Hydrogen Sulfide as an Emerging Gasotransmitter....1

1.3. Hydrogen Sulfide Storage: Acid-Labile and Bound-Sulfane Pools....3

1.4. Enzymatic Production of Hydrogen Sulfide....4

1.5. Cystathionine y-lyase (CSE) and Hydrogen Sulfide in the Cardiovascular System....5

1.6. Cystathionine β-synthase (CBS) and Hydrogen Sulfide in the Nervous System....7

1.7. 3-Mercaptopyruvate sulfurtransferase (MST) and Cysteine amino transferase (CAT)....9

1.8 Biology of Protein S-Sulfhydration (Persulfidation)....9

1.9. Methods to Detect Protein S-Sulfhydration....11

1.10. Methods to Detect Free Hydrogen Sulfide....12

1.11. Cysteine Biosynthesis via Reverse Transsulfuration....14

1.12. Cysteine Drives Endogenous Hydrogen Sulfide Production....15

1.13. PIP_2 Activation of Kir Channels....17

1.14. Role of Hydrogen Sulfide on Kir Channels....26

Chapter 2. Materials and Methods

2.1. Materials and Reagents....32

2.2. Molecular Biology....32

2.3. Electrophysiology....33

2.4. NaHS Treatment in TEVC Experiments.....34

2.5. Wortmannin (Wort) Treatment and Recording in TEVC Experiments.....34

2.6. Inside-out Macropatch Experiments.....37

2.7. NaHS Treatment in Macropatch Experiments.....37

2.8. TAG Switch Assay.....38

2.9. Molecular Dynamics (MD) Experiments.....39

3.0 Statistics.....40

Chapter 3. Hydrogen Sulfide Regulation of Kir Channel Activity is PIP_2-dependent and Mediated by Specific Cysteine Residues

3.1. Dual Role of NaHS on Kir Channels and Sulfhydration of Kir3.2 Channels.....41

3.2. NaHS Inhibition of Kir3.2* Channels is Dependent on Channel-PIP_2 Interactions.....42

3.3. Micromolar Concentrations of NaHS Inhibit Kir2.3 in Macropatch Recordings.....45

3.4. NaHS Inhibition of Kir3.2* Channels is Mediated by Sulfhydration of Specific Cytoplasmic Cysteine Residues.....46

3.5 CSE Co-expression Mimics Exogenous NaHS Effects on Kir3.2* Channels.....48

3.6 Molecular Dynamics Experiments Show Sulfhydration of Specific Cysteine Residues Alters Channel Gating and Interactions with PIP_2.....50

Chapter 4. Carbon Monoxide Inhibition of Kir2 and Kir3 Channels is also PIP_2-dependent and mediated by a Specific Cysteine Residue.....58

Chapter 5. Discussion.....63

Chapter 6. Future Directions.....68

Chapter 7. Literature Cited.....73

Vita.....83

List of Figures and Tables

Page

Figure 1. Dendrogram of the Kir family 18

Figure 2. Phosphatidylinositol (4,5)-bisphosphate and Dioctanoyl Phosphatidylinositol (4,5)-bisphosphate (diC8). 19

Figure 3. PIP_2 signaling pathway indirectly modulates ion channels through the activation of protein kinase C (PKC) and Calcium-dependent enzymes using secondary messengers. 20

Figure 4. Stimulatory effect of PIP_2 on Kir channels via direct regiospecific-electrostatic interactions 23

Figure 5. A Published crystal structure of Kir3.2 channel reveals direct channel-PIP_2 interactions 24

Figure 6. NaHS Incubation methodology 35

Figure 7. A schematic demonstrating inwardly-rectifying whole-cell potassium currents in *Xenopus laevis* oocytes using the ramp protocol 36

Figure 9: Exogenous Hydrogen Sulfide inhibits Kir3.x and Kir 2.x channels and activates Kir6.2 Currents 44

Figure 9. Hydrogen Sulfide Inhibition of Kir3.2 channel is altered by strengthening or weakening channel-PIP_2 interactions 47

Figure 10. Hydrogen Sulfide inhibition of Kir2.3 channel is mediated by micromolar concentrations of NaHS in macropatches 48

Figure 11. Specific cysteine residues are sulfhydrated in Hydrogen Sulfide regulation of Kir3.2* channels 52

Figure 12. Strength of channel-PIP_2 interactions is similar between Kir3.2* channels and Kir3.2* Cys-less mutant 53

Figure 13. Expression of CSE, an enzymatic producer of hydrogen sulfide, mimics NaHS effects 54

Figure 14. Molecular dynamics experiments provide mechanistic insight into how sulfhydration of specific residues on Kir3.2 channels affect channel-PIP_2 interactions and channel gating 55

Figure 15. Molecular dynamics experiments provide mechanistic insight as to how sulfhydration of C42 is permissive of Kir6.2 channel opening. 56

Figure 16: Figure 9. Carbon monoxide (CO) inhibition of Kir2.3 channels is PIP_2-dependent. 60

Figure 17. CO inhibition of Kir2.3 channels depends on Cysteine 28 (and not Cys 170) 61

Figure 18. CO Inhibits Kir2.3 channels in macropatches in a dose-dependent manner. 62

Table 1. Molecular dynamics experiments reveal direct changes in channel-PIP_2 interactions (Total contact between PIP_2 head group and channels, A.U.) 57

List of Abbreviations

aa-st PIP_2	Long chain-phosphatidylinositol-4,5-bisphosphate
C/A	Cell-attached
CAT	Cysteine amino transferase
cRNA	Complementary ribonucleic acid
CBS	Cystathionine β-synthase
CBL	Cystathionine lyase
CGS	Cystathionine Synthase
CSE	Cystathionine γ-lyase
CO	Carbon Monoxide
DAG	Diacylglycerol
DMSO	Dimethyl sulfoxide
DNA	Deoxyribonucleic acid
DTT	Dithiothreitol
diC8	Dioctanoyl phosphatidylinositol-4,5-bisphosphate
ED	Erectile dysfunction
GAPDH	Glyceraldehyde 3-phosphate dehydrogenase

HK	High potassium bath solution
H_2S	Hydrogen Sulfide
I/O	Inside-out
I/R injury	Ischemia reperfusion injury
IP_3	Inositol 1,4,5-trisphosphate
IRK3	Inwardly rectifying potassium channel 3
K_{ATP}	Adenosine-5'-tri-phosphate sensitive potassium channel
Kir	Inwardly rectifying potassium channels
LTP	Long term Potentiation
MMTS	Methanethiosulfonate
MSBT	Methylsulfonylbenzothiazole
MST	3-Mercaptopyruvate sulfurtransferase
NaHS	Sodium Hydrosulfide
NO	Nitric Oxide
NOS	Nitric Oxide Synthase
ND96K	High potassium bath solution
PLC	Phospholipase C
PI	Phosphatidylinositide

PI(4)P	Phosphatidylinositol-4-phosphate
PI(4,5)P_2	Phosphatidylinositol-4,5-bisphosphate
PIP5K	Phosphatidylinositol-4-phosphate 5-kinase
PKC	Protein kinase C
PKG-I	Protein Kinase G-I
PLC-γ	Phospholipase C gamma
PMA	Phorbol 12-myristate 13-acetate
PPG	DL-propargylglycine
PtdIns	Phosphatidylinositol
RNA	Ribonucleic acid
SAM	S-adenoysl methionine
SMC	Smooth muscle cells
Sulfhydration	S-Sulfhydration
TAG	Tag Switch Assay
TEA	Tetraethylammonium
TEVC	Two-electrode voltage clamp
WMN	Wortmannin

Abstract

HYDROGEN SULFIDE REGULATION OF KIR CHANNELS

By Junghoon Ha, M.S.

A dissertation submitted in partial fulfillment of the requirements for the degree of Doctor of Philosophy at Virginia Commonwealth University

Virginia Commonwealth University, 2018.

Major Director: Diomedes E. Logothetis, Former John D. Bower Chair, Department of Physiology and Biophysics

Inwardly rectifying potassium (Kir) channels establish and regulate the resting membrane potential of excitable cells in the heart, brain and other peripheral tissues. Phosphatidylinositol-4,5-bisphosphate (PIP_2) is a key direct activator of ion channels, including Kir channels. Gasotransmitters, such as carbon monoxide (CO), have been reported to regulate the activity of Kir channels by altering channel-PIP_2 interactions. We tested, in a model system, the effects and mechanism of action of another important gasotransmitter, hydrogen sulfide (H_2S) thought to play a key role in cellular responses under ischemic conditions. Direct administration of sodium hydrogen sulfide (NaHS), as an exogenous H_2S source, and expression of cystathionine γ-lyase (CSE), a key enzyme that produces endogenous H_2S in specific brain tissues, resulted in comparable current inhibition of several Kir2 and Kir3 channels. A "tag switch" assay provided biochemical evidence for sulfhydration of Kir3.2 channels. The extent of H_2S regulation depended on the strength of channel-PIP_2 interactions: H_2S regulation was attenuated when strengthening channel-PIP_2 interactions and was increased when channel-PIP_2 interactions were weakened by depleting PIP_2 levels via different manipulations. These H_2S effects took place

through specific cytoplasmic cysteine residues in Kir3.2 channels, where atomic resolution structures with PIP_2 gives us insight as to how they may alter channel-PIP_2 interactions. Mutation of these residues abolished H_2S inhibition, and reintroduction of specific cysteine residues into the background of the mutant lacking cytoplasmic cysteine residues, rescued H_2S inhibition. Molecular dynamics simulation experiments provided mechanistic insights as to how sulfhydration of specific cysteine residues could lead to changes in channel-PIP_2 interactions and channel gating.

Chapter 1: Background

1.1 Hydrogen Sulfide, Kir Channels, and Phosphatidylinositol 4,5-Bisphosphate (PIP_2)

The interplay of the biological gas Hydrogen Sulfide (H_2S), the inwardly rectifying potassium (Kir) channels, and the key signaling phospholipid phosphatidylinositol 4-5-bisphosphate (PIP_2) is the central theme of this thesis and lies at the hub of several independent research focuses that delineate their individual contributions in physiological and pathophysiological conditions. Our understanding of Kir channels, and their modulation by PIP_2, elucidates how these players may contribute to altering the excitability of specific cells. H_2S has more recently been burgeoned as a critical messenger molecule with a broad spectrum of significant physiological effects; yet we lack clear understanding about the cellular and molecular underpinnings behind its robust effects. The physiological roles of H_2S and various Kir channels, as well as the eventual convergence of these research tracts, will be described in the upcoming background sections.

1.2 Overview of Hydrogen Sulfide as an Emerging Gasotransmitter

Hydrogen sulfide (H_2S) is a colorless and flammable gas and has a molecular weight of 34.08 and vapor density (D) of 1.19, heavier than air (by definition has a D = 1.0) [1]. Having a boiling point of -60 °C, H_2S remains as a gas in physiological conditions (as well as in laboratory freezers in which H_2S aliquots are made in aqueous solutions and stored at -20 °C or -80 °C). At room temperature (20 °C), 1 gram of H_2S will dissolve readily in 242 ml H_2O. This gaseous molecule provides the bulk of the obnoxious odor one would notice emanating from rotten eggs and backed-up sewage well documented for its toxicity to humans in occupational as well as in

housing settings [2, 3], and is believed to be a major culprit leading to mass extinctions on earth in the end of the Permian period [4]. Given this catastrophic streak on mammalian existence, it is not surprising hydrogen sulfide was thought to be solely toxic until relatively recently. The production of H_2S in mammalian tissues, detected in mammalian tissues from human, rat, and cow in the range of 5-160 μM [5, 6], has been known for a long time; however, because of the toxicity connotation, it was largely ignored as a metabolic waste. While searching on Pubmed database for "Hydrogen sulfide" currently turns up more than 45,000 entries, very few actually examine the physiological importance or a beneficial role of H_2S to our body.

In the past four decades or so, the tides have turned for understanding the physiological role of hydrogen sulfide as it has garnered the reputation of a 'gasotransmitter' (to be discussed later), in the same company as the more traditional and established gaseous molecules like nitric oxide (NO) and carbon monoxide (CO) [7]. H_2S, like NO and CO, is also highly lipophilic (but to a lesser extent) and penetrates the bilayer of cell membranes at ease, having a membrane permeability index of 0.97 [1]. H_2S is essentially a weak acid in aqueous solution with an acid dissociation constant (pKa) of 6.76 at 37 °C and can dissociate into H^+ and hydrosulfide anion (HS^-), which in turn can dissociate into H^+ and sulfide anion (S^{2-}) [1].

$$H_2S \leftrightarrow H^+ + HS^- \leftrightarrow 2H^+ + S^{2-}$$

Given that the pK_{a1} is roughly 7.0 and the pK_{a2} is 17, there is essentially no S^{2-} in physiological systems (as it will not reach the basic pH of 17), leading to measurements of nearly equal amounts of H_2S and HS^- intracellularly, and approximately a 1:4 H_2S/HS^-

distribution in extracellular fluid and plasma under physiological conditions (pH 7.4 at 37°C) [1]. The half-life of dissolved H_2S in blood indicates it is more stable than NO in protein-free solutions; however, the physiological half-life may actually be shorter than measured by these experiments, as they can be scavenged by methemoglobin to form sulfhemoglobin as well as other proteins in plasma [1].

1.3 Acid-Labile and Bound-Sulfane Pools of Hydrogen Sulfide

Intracellular hydrogen sulfide reserves in various tissues are broadly categorized as: 1. Acid-labile sulfur or 2. Bound-sulfane sulfur [8-10]. Acid-labile sulfur, also known in the field as 'brain sulfide,' is released under acidifying conditions from iron-sulfur complexes of mitochondrial enzymes [1]. This pool of sulfur was elucidated through the detection of released hydrogen sulfide from rat brain homogenates when subjecting them to acidic solutions [11]. The physiological relevance of acid-labile sulfur is being contested as the optimal pH for sulfur release from this storage is < 5.4, whereas mitochondrial pH is generally between 7-8 [1]. In addition, acid-labile sulfur is difficult to measure directly because iron-sulfur complexes are unstable [1]. Bound-sulfane sulfur, characterized by covalent bonds between the sulfur atom with its six valence electrons and other sulfur atoms, was detected when additional hydrogen sulfide was released when experimenters subjected acid-treated brain homogenates with dithiothreitol (DTT), a small-molecule redox agent that would supply a reducing condition to cleave disulfide (S-S) covalent bonds [11]. The amount of hydrogen sulfide detected upon additional DTT-treatment was shown to be about the same as released by the acid, HCl, alone. In addition, experimenters showed that exogenous hydrogen sulfide was stored in the pool of bound-sulfane and not acid-labile pools of sulfur, as acid treatment did not release additional hydrogen sulfide in hydrogen sulfide-pretreated brain homogenates [11]. Sulfane sulfur is quantified by cold

cyanolysis and colorimetric measurement of ferric thicyanate [1]. So far, direct measurement of hydrogen sulfide levels has been elusive using two technologies: gas chromatography analysis of head-space gas or methylene blue spectrometry methods that would not differentiate acid-labile sulfur from bound sulfane sulfur [12].

The existing forms of bound-sulfane isolated from tissue include persulfides (R-S-SH), thiosulfates (S_2O_3)^{2}, thiosulfonate (R-S-SO_2-R), polysulfides (RS_nR, R is alkyl or aryl), polythionates ($S_nO_6^{2}$), elemental sulfur (S_8), and disulfides which have an unsaturated carbon adjacent to the C-S bond [7]. The persulfide (R-S-SH) forms of bound-sulfane can occur when exposed cysteine residues in a given protein are directly sulfhydrated and thereby, have become a candidate focal points for determining how hydrogen sulfide may affect protein activity [7]. The next section will discuss the enzymes that catalyze the sulfhydration of these cysteine residues.

1.4 Enzymatic Production of Hydrogen Sulfide

Most of endogenous hydrogen sulfide production occurs enzymatically, whereas only a small fraction is generated through the non-enzymatic reduction of elemental sulfur to hydrogen sulfide (using reducing equivalents obtained from glucose oxidation) [1]. The major impetus to understand the role of H_2S in physiology, as opposed to merely its toxicological effects, came after several experiments revealed that H_2S is ubiquitously generated from L-cysteine by several tissue-specific principal enzymes (analogous to the production of NO by nitric oxide synthase): cystathionine β-synthase (CBS), cystathionine γ-lyase (CSE), and 3-mercaptopyruvate sulfurtransferase (3-MST) / cysteine amino transferase (CAT). H_2S thereby signals via

sulfhydration, which is a post-translational modification of reactive cysteine residues, analogous to N-nitrosylation by nitric oxide [1, 7, 13, 14].

1.5. Cystathionine γ-lyase (CSE) and Hydrogen Sulfide in the Cardiovascular System

Cystathionine γ-lyase (CSE), also known as "cystathionase" or "cysteine lyase," is expressed as two isoforms of CSE in humans (alternatively spliced products that are different by 132 base pairs) and is a homotetramer consisting of 63 kDa subunits. CSE is expressed predominantly in the cardiovascular (CV) system, the respiratory system, liver, kidney, uterus, placenta, pancreatic islets, selective areas of the stomach, small intestine, as well as specific neuronal tissue in the brain [1, 7, 13, 14]. CSE binds L-cysteine as its substrate and several sulfur-containing co-substrates and uses pyridoxal-phosphate PLP, an active form of vitamin B6.

The finding that CSE is widely expressed in the cardiovascular system chiefly motivated several researchers to focus on the role of H_2S in the cardiovascular system, leading to the design of *in-vivo* and *in-vitro* experiments that interfered with endogenous production of H_2S and/or added exogenous H_2S to cardiovascular tissue/cells, using H_2S donors like L-cysteine or H_2S salts like sodium hydrogen sulfide (NaHS) and sodium sulfide (Na_2S) [7, 14]. These studies have led to the striking discovery that H_2S confers protection to the heart through diverse processes: combating cellular necrosis, apoptosis, oxidative stress, inflammation, as well as through the promotion of angiogenesis and regulation of mitochondrial respiration [13].

To better understand the broad role of CSE in mammals, two research teams from Canada and the United States spent 5 years to develop CSE-KO mice and test their phenotype [15]. This seminal work concluded in 2008 presents several major advancements in H_2S research. These experiments first showed that most, if not all, the hydrogen sulfide production in

the CV system is mediated by CSE. The most noticeable phenotype in CSE-KO mice was that they developed hypertension with an onset of 8 weeks. Lack of endogenous H_2S production is most likely the major reason since injection of exogenous H_2S into these mice rescued them from hypertension [15]. They also showed that the hypertension was due to severely damaged endothelium-dependent relaxation of small resistance arteries (in contrast to relaxation of larger arteries by carbon monoxide and nitric oxide gases) [15]. The authors' explanation for how hydrogen sulfide stimulated vasodilation is as follows: vascular endothelium generates H_2S via CSE action, and the newly produced hydrogen sulfide then produces additional H_2S in a positive-feedback mechanism involving the activation of muscarinic receptors and calmodulin stimulation. The H_2S, generated in this loop, then diffuses over to both endothelial and vascular SMCs to induce vasorelaxation. This described mechanism is very distinct from that of another EDRF, NO, and will be more thoroughly described in the background section that focuses on hydrogen sulfide effects on Kir channels [7, 14].

Interestingly, overexpressing CSE, or otherwise increasing the production of hydrogen sulfide, has a direct cardioprotective effect when the myocardium is deprived of oxygen and undergoing ischemic insults. More specifically, overexpressing CSE in the myocardium has also been shown to limit mouse cardiac ischemia-reperfusion damage (reduced myocardial infarct size) due to increased endogenous hydrogen sulfide levels [16]. Other effects from altered CSE expression and changed H_2S levels have been demonstrated in inflammation, atherosclerosis, diabetes, asthma as well as in erectile dysfunction (ED) [17-22].

1.6. Cystathionine β-synthase and Hydrogen Sulfide in the Nervous System

Cystathionine β-synthase (CBS) was first isolated by Braunstein et al. in 1969 as a serine sulfhydrase [23]. Like CSE, the N-terminal domain of CBS contains binding sites for both PLP and heme (protoporphyrin IX) [24]. The heme domain in CBS coordinates to both histidine and cysteine amino acids as axial ligands, in humans and rodents, and has been suggested as the enzyme's redox sensor, because deletion of the domain renders CBS insensitive to oxidative stress [25]. The carboxy-terminus of CBS contains an autoinhibitory domain of 140 residues, and binding to S-adenosyl methionine (SAM), the common co-substrate involved in methyl transfers, transmethylation, transsulfuration, and aminopropylation pathways, removes the autoinhibition [26]. Just as with CSE, CBS catalyzes the production of H_2S using L-cysteine (as well as homocysteine). The best characterized reaction catalyzed by CBS is the condensation of homocysteine and serine: L-serine + L-homocysteine to form cystathionine and water, which can also feed into the biosynthetic production of hydrogen sulfide [1, 7, 14].

CBS expression is significant in the brain as the primary physiological source of H_2S in the central nervous system [1, 7, 13, 14]. Unlike CSE, CBS expression is rare or absent in the cardiovascular and respiratory systems, testes, adrenal, and spleen in rats, mice, or humans. Initial studies showed that CBS was found to be highly expressed throughout the brain, especially in the hippocampus and cerebellum, when compared with the cerebral cortex and brain stem. In contrast, Enokido et al argued that CBS is preferentially expressed in astrocytes rather than neurons, which is verified by more thorough combined biochemical and histological examination, as well as more sensitive in situ hybridization techniques [1, 7, 14]. Recent findings suggest that CBS mainly localizes to astrocytes (and very specific hippocampal and striatal

neurons) [7]. Additionally, one study showed the basal hydrogen sulfide level in unstimulated human astrocytes is 3.0 μmol/g protein, 7.9-fold higher than in cultured microglia [27].

Analogous to the H_2S experiments that revealed the role of the gas in cardiovascular vasodilation, breakthrough findings linking the H_2S levels and functional changes in the brain, occurred when Abe and Kimura reported that H_2S donor, NaHS, facilitated the induction of hippocampal long-term potentiation (LTP) at micromolar concentrations [28]. This effect revealed the physiological role of hydrogen sulfide in the brain contrary to the toxic connotation it generally holds. The expression of CBS mRNA in the hippocampus using Northern blots [28] was further confirmed. Pharmacological manipulation of CBS activity altered H_2S production correspondingly [28]. Although it was not known up to that time whether altering endogenous H_2S level affects the long-term potentiation (LTP) process, a "neuromodulatory" role of exogenous H_2S in the brain was then first described.

Unfortunately, generating homozygous knock-outs (KOs) of CBS proved to be fatal to the mouse, yielding very little information compared to the CSE knockout mice, except that it is vital to the development of the mouse's brain as their life span was about 4 weeks [29]. Generation of heterozygous (HT) mice presented with the hyperhomocysteinemia phenotype, twice the normal homocysteine level, one of the substrates of CBS [29]. However, it was difficult to probe for the role of CBS and the hydrogen sulfide it produces, given that endogenous hydrogen sulfide production was still significant in the heterozygous mice in these experiments [29]. There is evidence that altered expression of CBS (and endogenous hydrogen sulfide) *in vivo* leads to various neurodegenerative diseases while replenishment with exogenous H_2S reversed the pathology [1].

1.7 3-Mercaptopyruvate sulfurtransferase (MST) and Cysteine amino transferase (CAT)

Mercaptopyruvate sulfurtransferase (MST) and cysteine amino transferase (CAT) also enzymatically produces hydrogen sulfide, but defects in MST do not lead to life-threatening phenotypes in mammals as altered CBS or CSE activity [1]. In the brain, MST was shown to be localized to the hippocampal pyramidal neurons, cerebellar purkinje cells, and mitral cells of the olfactory bulb. Also, MST was shown to be predominantly localized in proximal tubular epithelium of kidney as well as pericentral hepatocytes in the liver [30]. Like CBS and CSE, MST and CAT utilizes PLP as a cofactor, but MST uniquely relies on zinc as a cofactor. In cells, MST and CAT have been localized in cytosol and mitochondria [31]. Cooperatively, CAT converts L-cysteine to 3-MP, and MST transfers sulfur from 3-MP to a bound sulfide or other sulfur acceptors to form elemental sulfur [32]. The direct outcome of the pathway is the production of sulfane sulfur (or bound sufur). H_2S will be formed through reduction of atomic sulfur or releases from this bound sulfur, either in the thiosulfate or persulfide form. Although it is clear in *in-vitro* experiments that CAT/MST generates hydrogen sulfide, the physiological role of CAT/MST still remains unclear as experiments on CBS or CSE knockout mice, in which exposing rat liver and kidney cells to exogenous L-cysteine in CSE K/O mice failed to produce meaningful hydrogen sulfide in experiments [33]. In addition, the measurement of 3-MP, the only known sulfur donor for MST is elusive and has not been detected in-vivo, given its instability [1].

1.8. Biology of Protein S-Sulfhydration (Persulfidation)

Recently, hydrogen sulfide has been shown to signal through the covalent modification of cysteine residues through S-sulfhydration (or persulfidation) or the conversion of cysteine –SH

groups to hydropersulfide (-SSH groups) [7, 14]. S-sulfhydration (also referred to as "short-term as sulfhydration") is analogous to S-nitrosylation which occurs between NO molecules and cysteine residues of targeted proteins [7, 14]. Although there are remarkable similarities between S-sulfhydration and S-nitrosylation, there are several key differences: about 10-25% of endogenous glyceraldehyde 3-phosphate dehydrogenase (GAPDH), beta-tubulin, and actin are S-sulfhydrated *in vivo* whereas only about 1-2% of coverage may be applicable to NO [7, 14]. The functional outcome of S-sulfhydration and or S-nitrosylation may be distinct. For example, in the case for GAPDH activity, S-sulfhydration has been attributed to increases in functional activity whereas N-nitrosylation appears to decrease protein activity [34]. The GAPDH protein, for example, has sixteen cysteine residues that may be subjected to post-translational modification. GADPH activity has been shown to increase either through overexpression of CSE or direct application of hydrogen sulfide [34]. On the contrary, incubating purified GAPDH with NO modified its four cysteine residues per molecule, leading to the abolishment of its activity [35]. Studies have also shown that S-sulfhydration is more stable relative to S-nitrosylation, which makes it easier to detect via mass-spectrometry [1]. Also, S-sulfhydration occurs under resting conditions without the requirement of additional physiological stimulation, evidenced by the reduction of GADPH sulfhydration in CSE-KO mice and endogenous hydrogen sulfide production in CSE-KO mice, despite the fact that GADPH was unchanged [34]. In contrast, basal S-nitrosylation remained unchanged when all NOS enzymes, neuronal NOS (nNOS), eNOS and iNOS were knocked out in mice [35].

A requirement for S-sulfhydration is the availability of free thiol (–SH) groups. If oxidizing conditions cannot be met and the existence of disulfide bonds blocks the access of hydrogen sulfide to sulfhydryl groups, a two-step process could be involved [7]. Hydrogen

sulfide could disrupt disulfide bonds within proteins by acting as a reducing agent, which would expose free SH groups [7]. Then, another hydrogen sulfide molecule could bind exposed SH group and lead to S-sulfhydration. The prospect of competition occurring between H_2S and NO on the same exposed cysteine residue and thereby differentially altering protein function is an intriguing topic not properly addressed experimentally. Also, no endogenous desulfhydration molecule has been discovered for S-sulfhydration analogous to how *S*-nitrosylation can be reversed by denitrosylation with thioredoxins [36]. H_2S itself may also function as a desulfhydration molecule due to its reducing property the same way it has been shown to reduce disulfide bonds under specific circumstances. Or this desulfhydration role may also be performed by other capable endogenous reducing molecules like glutathione [1].

1.9 Methods to Detect Protein S-Sulfhydration

So far, the most improved technique employed to detect S-sulfhydration is the TAG-Switch Assay. This assay uses methylsulfonylbenzothiazole (MSBT) to block all thiol groups, after which a reagent compromising a nucleophile and a biotin moiety is reacted with the protein solution. The nucleophile only recognizes the MSBT-bound persulfide groups and not the free thiol group, so that only sulfhydrated proteins are then enriched using streptavidin conjugates and then analyzed by western blotting. The MSBT can further be tethered to fluorophores or other reporter molecules instead of biotin for added sensitivity.

The TAG-switch Assay is the derivative of another technique, the Biotin Switch Assay, which was used to identify the bulk of S-sulfhydration experiments and therefore worth mentioning despite agreement in the field that it is not as reliable [37]. In this modified biotin switch assay, a variant of the assay developed to detect S-nitrosylation of proteins, the

sulfhydrated protein is treated with methyl methanethiosulfonate (MMTS) to block specifically unmodified cysteine residues. In this technique, a control reaction is treated with dithiothreitol (DTT) to reduce persulfide groups, and then blocked with MMTS. After removal of excess MMTS, the samples are labeled with biotin, which interacts with the thiol group. The biotinylated proteins are enriched by affinity capture using streptavidin conjugates, which specifically bind to biotinylated proteins, and then analyzed by western blotting [7]. The control samples treated with DTT, where the persulfide group is reduced back to the corresponding thiol, will not yield a signal on western blots. The major issue with this technique has been the findings that in the hands of many investigators MMTS would also label the free thiol-groups, which produced a great deal of false positive results and therefore is no longer the standard technique for measuring S-sulfhydration [37]. Therefore, in a gamut of these studies, the positive results were corroborated by mass spectrometry to detect specific modification of cysteine residues [7].

1.10 Methods to Detect Free Hydrogen Sulfide

The physiological range of H_2S in the circulation has been estimated at 10 –100 μM in healthy animals and humans [38-41]. Interestingly, this circulating H_2S amounts seem unaffected by aging. A study revealed no change in serum H_2S concentration among three age groups of humans spanning 50-80 years of age (34 –36 μM) [42]. In rat, mouse, and rabbit blood plasma, H_2S was detected at micromolar ranges as well has been reported in many other vertebrates [1]. Endogenous levels of H_2S in rat brain homogenates are 50–160 μM [1] . Similar H_2S levels were reported in the liver, kidney, and pancreas [1] . H_2S production was clearly measured in the cardiovascular system [41, 43].

Measurement of hydrogen sulfide in animal serum is and remains a complicated technical matter. Whereas there is agreement to the hydrogen sulfide ranges detected in most studies *in-vivo*, efforts to detect hydrogen sulfide levels *in-vitro* on specific tissue cell lines have revealed significantly lower ranges or sometimes even concluded that hydrogen sulfide cannot be detected**.** One explanation for these low values of H_2S *in vitro* is the rapid decay within 30 minutes of H_2S concentrations, from micromolar to undetectable levels [44]. Another related concern is the reliability of equipment used to measure the hydrogen sulfide themselves. The real-time polarographic sensor was initially developed by Doeller et al. in 2005 [45]. Using the same kind of house-made sensor, Benavides et al. [43] demonstrated that red blood cells produced H_2S. In two other studies using polarographic sensors, free H_2S concentrations in whole rat blood have been detected at 5 μM [45]. These experiments could have been helped by simultaneous employment of the polarographic sensor and other detection methods for H_2S detection validating the detection of H_2S in the serum. In contrast to the sulfur ion-selective electrode which detects total sulfur in the blood including its acid labile, bound, or free H_2S forms (discussed in the bound or unbound hydrogen sulfide section), the polarographic sensor is sensitive only to freely dissolved H_2S gas. It is possible that the readings are simply accurate and reflect the possible reality that significant amount of H_2S in circulation may not be in a free form as dissolved gas [1] .

Focusing on tissue-specific hydrogen sulfide production (rather than in serum), the gas chromatography technique also produced similar variances in hydrogen sulfide detection. Furne et al. [46] reported very low tissue production of H_2S in homogenized mouse brain and liver in the nanomolar range of concentrations. An interesting comparison for this observation is that

Hyspler et al. [39] also used gas chromatography-mass spectrometry (GC-MS) analysis and detected human whole blood H_2S levels at 35– 80 μM. Even using a polarographic sensor, others have detected significant tissue production of H_2S from the brain and liver [45].

Many of the current H_2S measurement techniques, such as spectrophotometry, chromatography, and ion-selective electrodes, were originally developed to meet the industrial demand for monitoring H_2S pollution in the environment. [1] These techniques are usually invasive and require a bulky quantity of samples, and they also do not take account for the conditions of biological studies, such as the existence of H_2S scavenging molecules, interference of hemoglobin or other pigment compounds, redox balance, pH changes, etc.

1.11. L-Cysteine Biosynthesis via Reverse Transsulfuration

Reverse transsulfuration describes the metabolic pathway in which methionine, an essential amino acid, is converted to cysteine in vertebrate and fungal species [47]. Whereas, transsulfuration is a term which describes the opposite interconversion process: the conversion of methionine from cysteine, catalyzed by cystathionine lyase (CBL) and cystathionine synthase (CGS) in plant and bacterial species [47]. Reverse transsulfuration contributes significantly to the intracellular pool of cysteine in mammals as they possess several flux-controlling enzymes to shift the equilibrium in favor of cysteine. This biosynthetic pathway serves as a catabolic machinery for the breakdown of methionine and its toxic intermediates including homocysteine, a major clinical marker for several human physiological disorders [48]. At elevated levels, homocysteine is an independent risk factor for cardiovascular diseases and other complex physiological disorders [48].

In addition to being the key product of reverse transsulfuration, cysteine is also used for biosynthesis of glutathione and is the primary substrate for hydrogen sulfide biosynthesis regulated by CBS and CSE, enzymes described earlier. CBS can also catalyze the condensation of homocysteine and serine to form cystathionine in an irreversible reaction favoring its hydrolysis by CSE to produce cysteine, alpha-ketobutyrate, and ammonia [48]. Thus, reverse transsulfuration describes the transfer of methionine sulfur to serine to synthesize cysteine. Tissues unable to conduct sufficient reverse transsulfuration, lacking the biosynthetic machinery, require exogenous source of cysteine and must be able to export homocysteine for further metabolism by other tissues [48]. There are severe physiological consequences due to buildup of metabolic intermediates, homocysteine as well as interrupted cysteine production.

1.12. Cysteine Drives Endogenous Hydrogen Sulfide Production

L-Cysteine is derived from the dietary amino acid methionine via reverse transsulfuration [1]. Although L-cysteine is classified as a non-essential amino acid, which means that mammals can biosynthesize L-cysteine under normal physiological conditions, major deficiencies in the biochemical (reverse transsulfuration) pathway, which converts methionine to cysteine, or lack of dietary methionine, an essential amino acid, will basically confer L-cysteine with the status of an essential amino acid [1]. In such circumstances, the burden of cysteine production will rely solely on the enzymes that sulfurylate O-acetylhomoserine to give homocysteine, which then joins the reverse transsulfuration pathway to be converted to cysteine [49]. Thereby, experimenters could lower L-cysteine levels, and thereby reduce endogenous hydrogen sulfide levels by depriving animals of methionine- or cysteine- containing diets. Several studies demonstrated that exogenous L-cysteine application limited the infarct size in ischemic heart, in

which the protective effect of L-cysteine was believed to be due to the enhanced endogenous production of hydrogen sulfide via CSE action [50]. Inhibition of CSE activity with DL-propagylglucine (PPG), an antibiotic produced by *Streptomyces,* applied simultaneously with PPG abolished the effect of L-cysteine [50].

However, not all biological effects of cysteine can easily be explained by production of hydrogen sulfide. The side chains of cysteine composed of non-polar thiol confers overall hydrophobicity to the amino acid. Used as a nucleophile, this thiol side chain has been shown to participate in various enzymatic reactions [1]. In addition, thiol-side groups when oxidized can form the derivative cystine, which plays a critical structural (and thereby functional) role in many proteins [1]. Addition of L-cysteine can increase the physiological pool of other sulfur-containing amino acids, especially cysteine, methionine, and S-adenosylmethionine, are of which are essential for the growth and activities of all cells [1]. For example, when CSE-KO mice were fed with cysteine-limited diets, they exhibited decreased levels of cysteine, glutathione, and hydrogen sulfide and most notably increased plasma homocysteine levels [51]. Animals presented with growth retardation and shortened life span with their cause of death being tied to paralysis of upper extremities and skeletal muscle atrophy [52]. Injecting CSE-KO animals with NaHS daily did not reverse or stop the cysteine-limiting diet induced decrease growth retardation of CSE-KO mice [52]. Only reintroducing cysteine to their diets allowed the animal to recover from these developmental events[52]. Experimenters thus concluded that CSE is required for cysteine biosynthesis and that sufficient cysteine supply is a prerequisite ensuring normal growth development of mice in the absence of the CSE enzyme in these animals.

1.13. PIP_2 Activation of Kir Channels

Inwardly rectifying potassium channels (Fig. 1) establish and regulate the resting membrane potential of excitable cells in tissues such as brain and heart. A wealth of electrophysiological, structural, and biochemical studies has revealed that a biological phospholipid, phosphatidylinositol 4,5-bisphosphate (PIP_2), is a key direct activator of Kir (inwardly-rectifying K^+) channels. Direct phosphoinositide control of the activity of ion channels has emerged as a critical molecular theme concerning the activation of Kir (inwardly rectifying K^+) channels. Various experiments on Kir channels have revealed the critical role of a specific phosphoinositide, phosphatidylinositol 4,5-bisphosphate (PIP_2) in their gating. Several post-translational modifications, such as phosphorylation of specific residues, have been shown to directly or allosterically alter K^+ channel interaction with PIP_2 [53, 54].

PIP_2 is a signaling phospholipid (Fig. 2) and has been increasingly appreciated in the past years: first as the precursor of ubiquitous downstream signals (inositol-trisphosphate IP_3, diacylglycerol DAG, and PIP_3), later serving a role in membrane localization of proteins in different membranous compartments, and more recently as a direct modulator of the activity of transmembrane proteins, such as ion channels and transporters [55-57]. In the intervening years, researchers showed that most ion channels tested to date depend on adequate PIP_2 levels to maintain their activity, suggesting a conserved mechanism by which ion channel function is regulated by PIP_2. Co-crystal structures of inwardly rectifying K^+ (Kir) channels with PIP_2 have highlighted the nature of the direct interactions of $PI(4,5)P_2$ at a key position capable of modulating two of the channel gates, the helix bundle crossing (HBC) and the cytosolic

Figure 1. Dendrogram of the Kir family. The Kir superfamily contains at least 15 members in six distinct subfamilies (Kir1, Kir2, Kir3, Kir5, Kir6, Kir7) that respond to various cytoplasmic and extracellular modulators; channels are two-membrane spanning (2TM) and share about 30-40% homology among the Kir subfamilies and >60% within the subfamilies. Kir channels were characterized strictly by their electrophysiological behavior as they allow more conduction in the inward than in the outward direction due to reduced open probability in depolarizing conditions across the membrane. However, in physiological conditions, Kir channels have a key role in stabilizing the membrane potential. In addition, regulation of these channels can alter the membrane potential and cellular excitability.

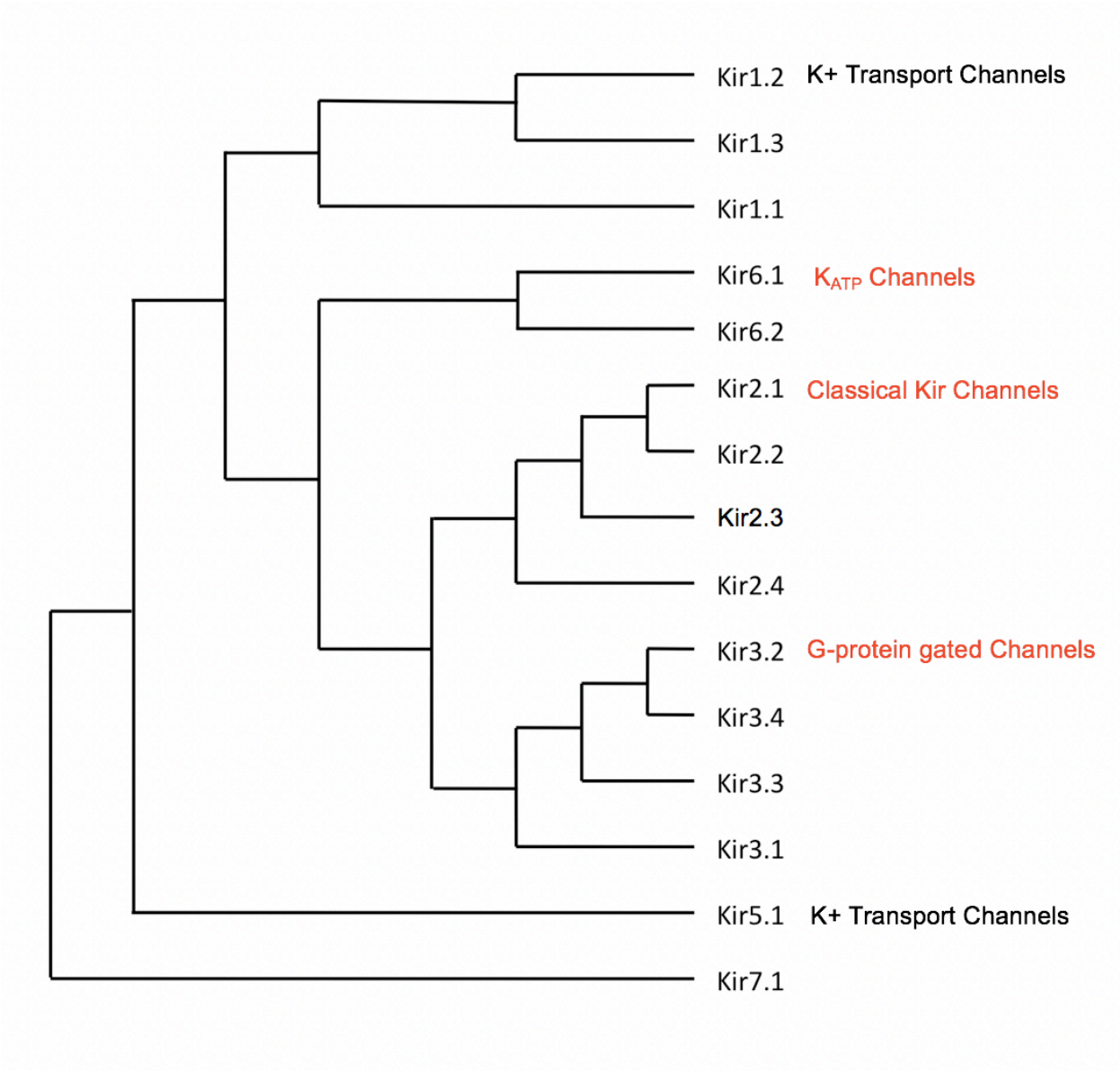


Figure 2. Phosphatidylinositol (4,5)-bisphosphate and dioctanoyl PI(4,5)-bisphosphate (diC8). PtdIns(4,5)P_2 is a minor phospholipid component of the cytoplasmic leaflet in plasma membranes, where it is a significant substrate for a number of membrane-localized signaling proteins. PtdIns(4,5)P_2 is primarily made by the type I phosphatidylinositol 4 phosphate 5 kinases from PI(4)P. **A. Long-chain aa-st PI(4,5)P_2.** Schematic of endogenously produced PI(4,5)P_2. **B. Soluble dioctanoyl PI(4,5)P_2 (diC8).** Schematic of chemically modified PI(4,5)P_2. The palmatoyl group and 19-carbon long chain of aa-st PI(4,5)P_2 have been replaced by shorter, more soluble singly-bonded 8-carbon long fatty acid chains.

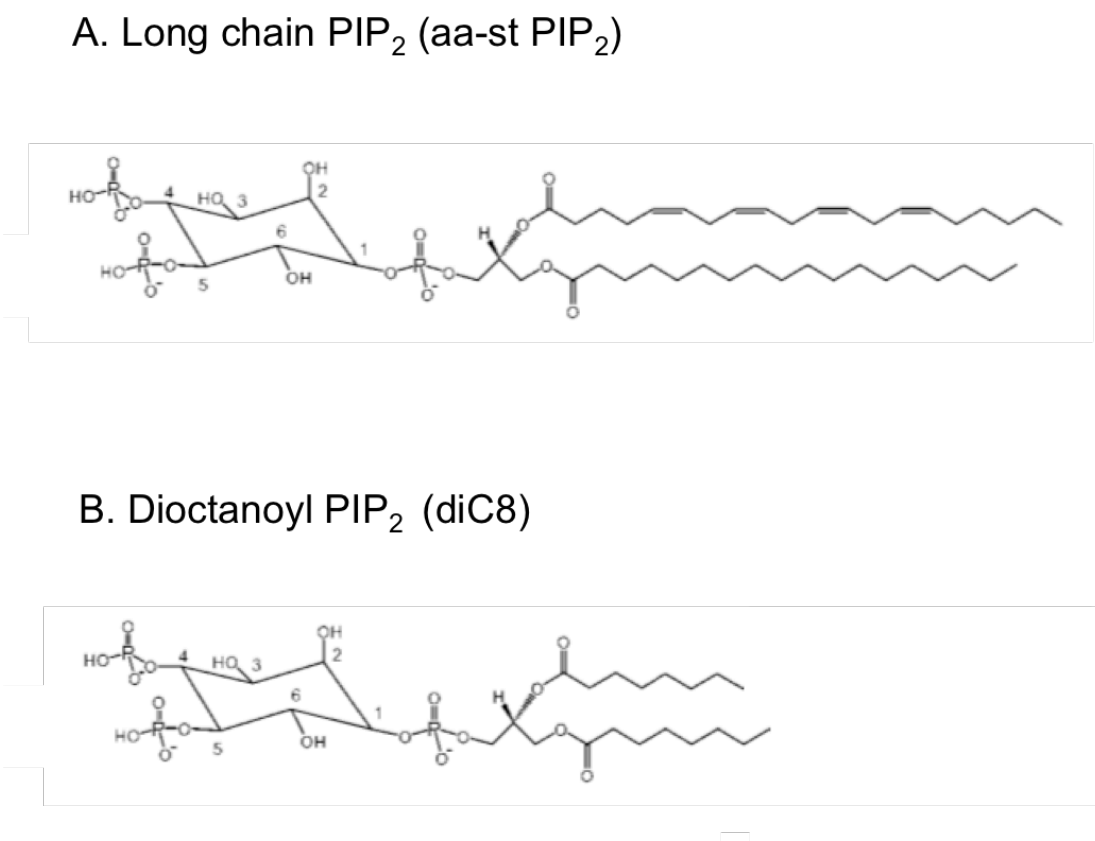
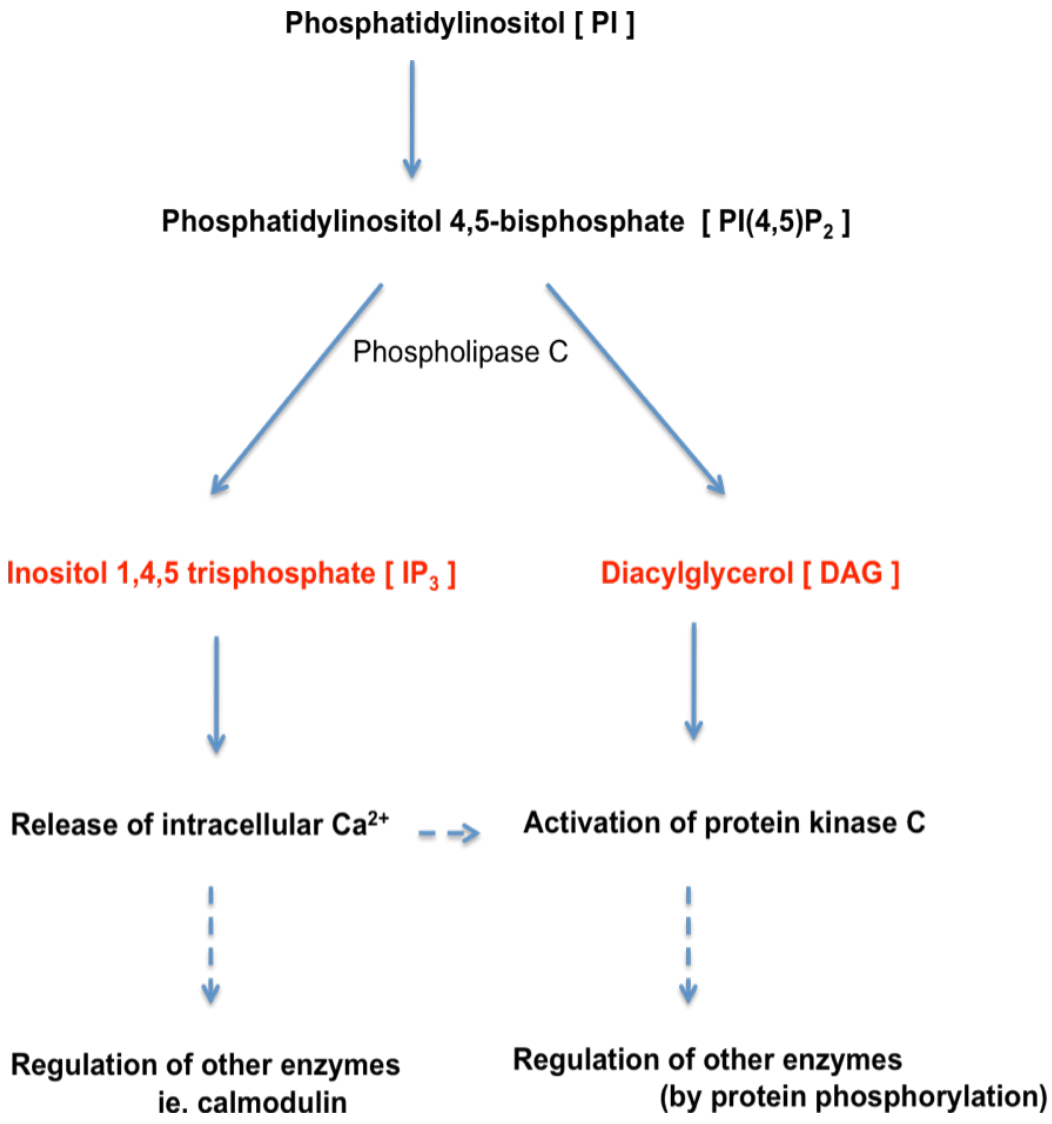


Figure 3. PIP_2 signaling pathway indirectly modulates ion channels through the activation of protein kinase C (PKC) and Ca^{2+}-dependent enzymes using secondary messengers. Activation of phospholipase C (PLC) results in the hydrolysis of phosphatidylinositol (PIP_2) to produce inositol 1,4,5-triphosphate (IP_3) and diacylglycerol (DAG). IP_3 activates Ca^{2+} channels in the endoplasmic reticulum (ER) triggering the release of Ca^{2+} from intracellular stores. The cytoplasmic rise in Ca^{2+} level and DAG then activate protein kinase C (PKC), which in turn phosphorylates K^+ channels, thereby modulating current across the membrane.



or G-loop gates. Ever since, direct phosphoinositide control of the activity of ion channels has emerged as a critical molecular theme concerning the activation of Kir (inwardly rectifying K^+) channels.

Prior to the crystal structures, a flurry of electrophysiological experiments on Kir channels had corroborated the critical role of a specific $P(4,5)P_2$ in their gating. Hilgemann and colleagues demonstrated that phosphoinositides, highly negative-charged anionic lipids with myo-inositol in the head group can also directly modulate channel activity [56]. Their experiments revealed that phosphoinositides such as phosphatidylinositol-4,5-bisphosphate (PIP_2) can activate native cardiac K_{ATP} channels. Ensuing studies by Fan and Makielski [55] uncovered that PIP_2 modulation of ion channels was not only limited to K_{ATP} channels, but also applied to other inwardly rectifying potassium (Kir) channels such as Kir1.1 and Kir2.1, and these findings were eventually extended to all other members of the Kir family of channels. In the background of channel- PIP_2 interactions, several post-translational modifications on the Kir channels, such as phosphorylation of specific channel residues, have been shown to directly or allosterically alter Kir channel interaction with PIP_2 [53].

In general, phosphatidylinositol-4,5-bisphosphate, $PI(4,5)P_2$, was shown to be the most abundant and reliable of the phosphoinositides in activating Kir channels (albeit differentially) compared to other naturally occurring phosphoinositides: PI, PI(4)P, $PI(3,4)P_2$, $PI(3,5)P_2$ and $PI(3,4,5)P_3$ [58-61]. Although, the parent compound phosphatidylinositol (PI) can become phosphorylated at the 3, 4, and 5 positions of the inositol ring in every combination, $PI(4,5)P_2$ (Fig. 2) is the most abundant poly-phosphoinositol making up 1% of the total phospholipids of the plasma membrane [62]. PIP_2 has three phosphate groups, one of which is in a phosphodiester bond, and a net charge near -5 at neutral pH [63]. In the late 1970s, PIP_2 was shown to be the

substrate of plasma membrane-delimited enzyme phospholipase C (PLC), which hydrolyzes PIP_2 into two secondary messengers (Fig. 3), soluble inositol 1,4,5-trisphosphate (IP_3) and membrane-anchored diacylglycerol (DAG) [64]. IP_3 and DAG were subsequently shown to release Ca^{2+} from intracellular stores within the cell and to recruit and activate protein kinase C (PKC), respectively [63]. Moreover, PIP_2 was shown to serve as a targeting anchor for proteins that catalyze endocytosis and exocytosis such as GTPases, PKC, and other components of the actin cytoskeleton [64]. Since PIP_2 served as an epicenter for these two signaling pathways that affect ion channel function indirectly through secondary messengers, it became critical to perform the necessary control experiments to ensure that electrical phenotype was a result of direct PIP_2-channel interactions.

As PIP_2 direct activation of Kir channels became evident, researchers began focusing on where and how PIP_2 interacts with Kir channels. First attempts examined the effects of naturally occurring phosphoinositol lipids on cloned Kir6.2/SUR1, through their direct application to the cytoplasmic membrane side of excised patches [58]. Channel activity in these experiments was allowed to rundown, a process which typically occurs in excised patches due to hydrolysis and/or dephosphorylation of the endogenous phosphoinositide PIP_2. Several phosphoinositides were tested to see whether they could restore channel function. As $PI(4,5)P_2$ emerged as the most effective of the phosphoinositides in recovering (activating) channel activity, it became clear that Kir channels exhibited distinct affinities (as well as stereospecific requirements) with the phosphate groups on inositol carbon positions 4 and 5 [65]. Hypothesizing that the acidic negatively charged phosphates of PIP_2 (at neutral pH) interact electrostatically with basic positively charged residues on ion channels (Fig. 4), laboratories focused on identifying channel regions that are vital for ion-channel modulation by PIP_2.

Figure 4. Stimulatory effect of PIP_2 on Kir channels via direct regiospecific-electrostatic interactions. Two highly negative-charged phosphate groups (depicted here by red circles) attached to the 4 and 5 carbons of inositol (represented by hexagonal inositol ring) in the inner leaflet of the plasma membrane interact with candidate positively charged residues that are highly conserved in the Kir superfamily. Net inward movement of potassium ions depicted by the blue arrow is indicative of hyperpolarizing conditions typically applied to membranes expressing Kir channels. **A.** Schematic of a Kir channel in the inactivated closed state. When the level of PIP_2 is low (often depleted through PIP_2 dephosphorylation, hydrolysis, or run down in excised patch experiments), Kir channel remains in the closed state. **B.** Schematic of a Kir channel in the activated open state via the binding of PIP_2 to the channel: relies both on the spatial distribution of phosphate groups on the inositol ring as well as electrostatic interactions.

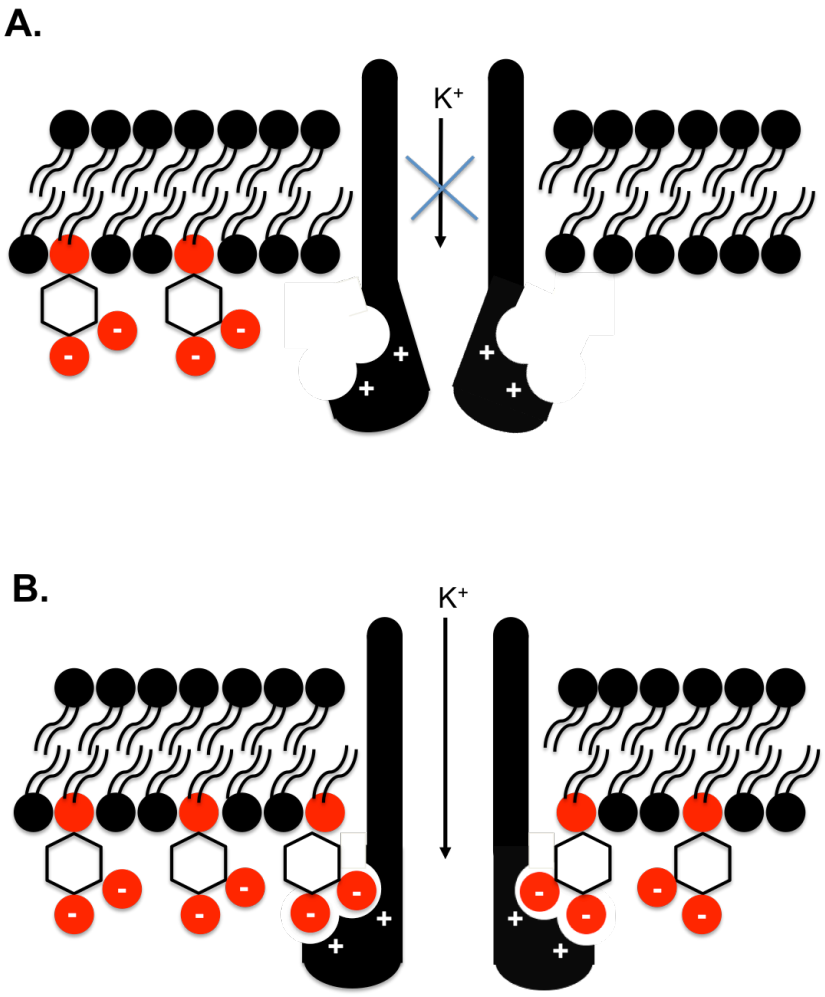


Figure 5. A Published Crystal Structure of Kir3.2 (GIRK2) Channel reveals direct Channel-PIP_2 Interactions. (Whorton et. al. *Cell* 2011). Side view of GIRK2 crystal structure(PDB code 3SYA). Labelled: M1 and M2 transmembrane helices, a selectivity filter, two gates: Inner-helix gate and G-loop gate, and turret, known region to bind toxins. **B. Key Positively-charged residues of GIRK2 channel involved in PIP_2 binding (shown in space-filing).** PIP_2 is represented as in stick molecule conformation (green arachidonyl and stearyl fatty acid chains).

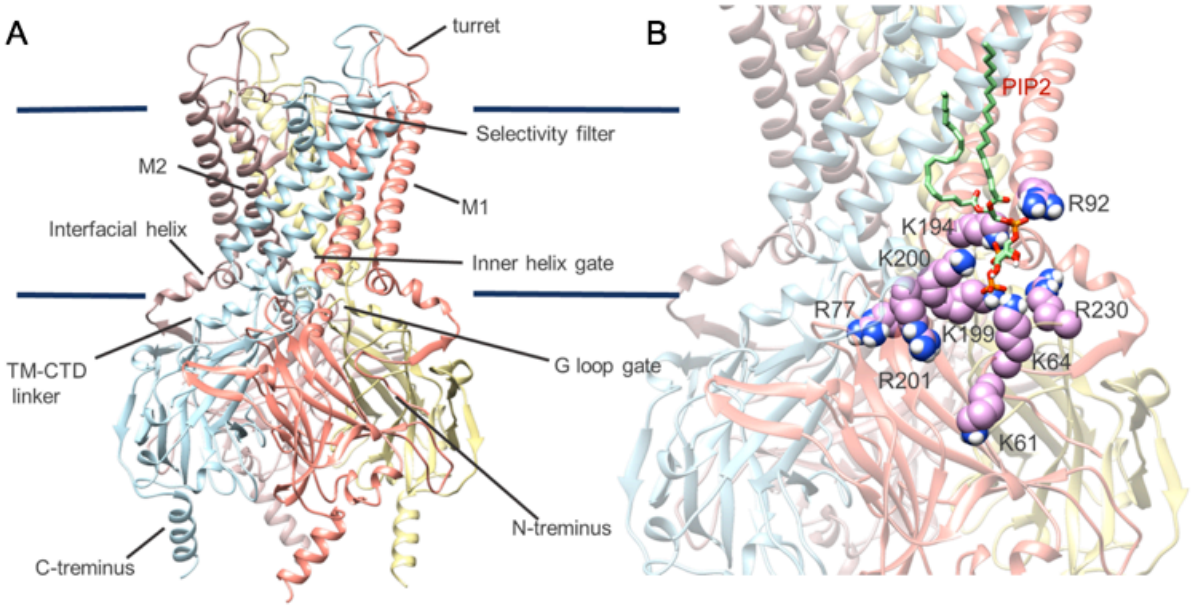


Figure adapted from *Whorton et. al. Cell* 2011 and generated by Dr. Yu Xu.

These electrophysiological patch experiments required the use of modified shorter PIP_2 analogs such as dioctanoyl PIP_2 (diC8) (Fig. 2), which due to their water solubility were much easier to wash out of membranes [65]. Logothetis and coworkers utilized diC8 to determine the apparent affinity of PIP_2 for a particular Kir channel and compare it to other channels [66, 67].

The conserved basic sites that bind PIP_2 were unveiled through systematic mutagenesis of highly conserved basic residues in the cytoplasmic domains of Kir channels [65]. Mutant channels, whose basic residues were replaced with neutral residues, exhibited decreased recovery of ion channel activity upon addition of exogenous PIP_2 to the cytoplasmic side. Furthermore, mutant channels showed increased sensitivity to inhibition by poly-L-lysine (a PIP_2 scavenger) as well as PIP_2 specific antibodies suggesting that the mutations reduced apparent PIP_2 affinity [68]. Subsequent experiments also showed that one could swap a mere residue in Kir2.3 with a corresponding residue in a related Kir channel (Kir2.1) (Fig. 1) that is more sensitive to PIP_2, to increase its apparent affinity to PIP_2 and vice-versa [69]. Interestingly, single point mutations in the pore helix of Kir3.x channels that exist physiologically as heterotetramers enhanced the activity and channel-PIP_2 affinity of various tissue specific homomeric Kir3.x channels when they are expressed heterologously (referred to as Kir*; where Kir3.1* has the F137S mutation, Kir3.4* or G4* has the S143T mutation or where Kir3.2* has the E152D mutation).

Methods were devised to alter cellular pools of PIP_2 such as the use of Wortmannin, a specific phosphatidyl-inositol 3-kinase (PI3K) inhibitor at nanomolar concentrations, when used at high micromolar concentrations can inhibit phosphatidyl-inositol 4- kinase (PI4K), reducing the available pool of PI4P (phosphatidyl-inositol 4-phosphate) for conversion into PIP_2 by PIP5K (phosphatidyl-inositol phosphate 5-kinase). The co-expression of PIP5K would on the other hand

increase the level of cellular PIP_2 in the cell. The co-expression of Ci-VSP, a voltage-activated PIP_2 5-phosphatase, allowed researchers to dynamically deplete PIP_2 levels at the membrane and concurrently assay the relative strength of channel-PIP_2 interactions by examining the kinetics and recovery of Kir channels (i.e. observe what happens to current as PIP_2 pools are reduced simultaneously [54, 70, 71]. Thus, our understanding of Kir channel modulation by PIP_2 has offered great insights into mechanisms underlying the gating of ion channels.

1.14. Role of Hydrogen Sulfide on Kir Channels

One of the major breakthrough experiments revealing a clear physiological role for hydrogen sulfide came in 2001 when Zhao et al. for the first time cloned the CSE gene from rat vascular tissues and demonstrated that both the expression and activity of CSE can be upregulated by NO, leading to increased production of H_2S from vascular smooth muscle cells (SMCs) [41]. The team also showed that, unlike NO that relaxes blood vessel walls by activating guanylyl cyclase to synthesize cGMP, the specific molecular targets of H_2S in vascular SMCs are K_{ATP} channels [41]. This is the first molecule target of H_2S identified in the cardiovascular system. By stimulating K_{ATP} channels, H_2S causes vasorelaxation within a physiologically-relevant concentration range [41].

In the many clinical research endeavors that sought to identify the role of hydrogen sulfide in cardiovascular diseases, hydrogen sulfide emerged as a therapeutic agent for ischemic heart disease, the pathophysiological state characterized by reduced blood supply to the heart and the most common cause of death in most western countries [72]. Thereby, navigating through the complex pathophysiology and exploring therapeutic measures pertinent to novel players like

H_2S became paramount to our efforts to better combat the disease. While, some of these diverse effects were simply attributed to H_2S altering the redox state of cellular environments [73], other profound effects are thought to take place via persulfidation of proteins (addition of persulfide -SSH moieties also described as S-sulfhydration), the post-translational modification of regulatory cysteine (Cys) residues (analogous to N-nitrosylation of proteins at Cys residues by the gas nitric oxide, NO) [1, 7, 14]. In these studies, the extent of protein persulfidation was detected previously by biochemical techniques, such as the Biotin Switch Assay [34], and the more recently accepted gold standard, the Tag Switch Assay (TAG) [37], as well as by mass spectrometry [74].

One seminal work actually bridged a specific persulfidation of a regulatory cysteine residue in an ion channel, K_{ATP} channel (Kir6.2 channel) to the enlargement (vasodilation) of blood vessels, demonstrating the striking influence of H_2S on an ion channel expressed in the cardiovascular system [75]. While lacking the same degree of clarity as to providing a mechanistic role for H_2S in vasodilation, experiments on rat myocardium *in-vivo*, showed that exogenous H_2S is able to confer cardioprotection and diminish the myocardial infarct size following ischemia and reperfusion (I/R) injury, either through pre-I/R [16, 76, 77] or post-I/R [78] treatment with exogenous H_2S. In agreement, endogenously induced H_2S, through the overexpression of protein kinase G (PKG-Iα), which increases CSE expression in the myocardium, also lead to cardioprotective effects following I/R injury [79]. Stunningly, the addition of a K_{ATP} channel blocker, glibenclamide, abrogated the beneficial effects of H_2S in both scenarios [77, 78]. It is unclear whether K_{ATP} currents, by hyperpolarizing myocardium affected by ischemia, permit the beneficial effects of H_2S, or whether the role of H_2S is to directly activate K_{ATP} and through this mechanism (mainly) reduce the extent of damage by I/R

injury. Such findings strongly make the case for understanding how alterations in cell excitability by H_2S may contribute to physiological effects that are beneficial (or harmful) to the cardiac tissue (atria and ventricles).

It is also well established that the activation of K_{ATP} channels (Kir6.2 channels) in the myocardium has been shown to play a pivotal role in cardioprotection during I/R injury (independent of exogenous H_2S treatment) and is a crucial component of the phenomenon termed cardiac ischemic pre- conditioning [80]. Overall, these results describe the clinical beneficial effect of H_2S when Kir6.2 channels are active, setting the stage for us to understand the mechanistic details of how H_2S persulfidation activates Kir6.2 channels in the heart as well as to explore whether it targets other ion channels, especially other closely related members of Kir (inwardly rectifying K^+) channels that are widely distributed in the myocardium (i.e. Kir 2.x, and Kir3.x channels) [81]. If H_2S does affect Kir channels at large, the gaseous molecule would further orchestrate the passive and active electrical properties of the heart drawing attention to differential expression of such target ion channels in the myocardium (in atrial or ventricular tissue) as well as the potential pharmacological profile of H_2S for activating these ion channels. Physiologically, inhibition of Kir channels would cause depolarization of cardiac tissue (elevating the resting membrane potential to more positive values), lead to several electrophysiological phenotypes such as lengthening of the action potential duration (APD), whereas, conversely, activation of Kir channels would result in hyperpolarization of cardiac cells (depressing the resting membrane potential), and lead to shortening of the APD [81].

There is already some evidence of classical Kir (Kir2.x) channel inhibition by another established gasotransmitter, carbon monoxide (CO), marked by prolonging the action potential

duration (APD) of rat cardiac ventricular myocytes [82]. It was also shown in normal rats, not subjected to pathological *in-vivo* models, H_2S administered through NaHS and Na_2S led directly to decreases in heart rate (HR), cardiac output (CO) despite systemic decreases in peripheral resistance [83], which show the direct effects of H_2S on the heart itself apart from compensatory cardiovascular mechanisms (in which HR and CO would increase in response to decreased peripheral resistance). Consistent with the *in-vivo* results in normal rats, cardiomyocytes of ventricular, atrial, and nodal subtypes differentiated from H9 embryonic stem cells (hESCs) and human induced pluripotent cells (hiPSCs) also showed slowing of cardiomyocyte contraction rates when exposed to a range of exogenous H_2S delivered with NaHS [84]. However, the apparent beneficial effects of H_2S on I/R reperfusion injury models are not always consistent, especially when it comes to higher doses of NaHS. For example, in one study, a dose of exogenously applied NaHS was shown to be cardioprotective, whereas applying a higher dose did not confer any beneficial effects to the irreversible injury [77]. Another experiment showed that extended NaHS perfusion also led to desensitization of H_2S effects [83] without offering an explanation. In addition, H_2S has been shown to have a starkly damaging effect when it comes to ischemic insults to the brain [85], a distinct tissue type with differential expression of ion channels.

In summary, the contribution of Kir channels, other than probing the role of Kir6.2 through the co-application of glibenclamide, has not been studied. Experimenters attempted to assess Kir contribution using tetraethylammonium (TEA), a non-specific K^+ channel blocker, and used channel blocker concentrations insufficient to block members of the Kir family of channels [83] . The mechanistic details underlying the conflicting effects by H_2S need to be reconciled in order for hydrogen sulfide to be reliably used as a therapeutic agent to treat cardiac

pathologies such as I/R injury. Moreover, we do not understand why H_2S hyperpolarizes cardiomyocytes [75, 84] whereas it depolarizes cerebral components [86-89] within a certain range of concentrations. For example, a diverse subtype of neurons been shown to depolarize upon exposure to H_2S: subfornical organ (SFO) neurons [88], trigeminal ganglion (TG) neurons [86], hypothalamic paraventricular neurons [89], as well as intact tissue such as in entorhinal cortex slices [87] and nucleus of the solitary tract [90]. In addition, we lack a clear understanding of exactly how H_2S is able to offer protective effects in cardiac ischemia whereas it is punishing to neuronal tissue undergoing cerebral ischemia, and the role of changed excitability of these tissues in their respective pathophysiology needs to be addressed. In particular, the effect of H_2S on Kir channels needs to be explored given that resting membrane potential changes and thus cell excitability depends largely on Kir channels, and some changes in their response to H_2S can be attributed directly to H_2S-Kir channel effects. Because H_2S appears to depress the excitability of the heart, whereas it increases the excitability of other tissues like the brain, worsening seizure-like symptoms, the thorough examination of ion channel targets other than Kir6.2 channels is critical as well as pinning down the mechanisms underlying their modulation.

One theme emerging from these studies is that H_2S increases the excitability of neuronal compartments [86-90], whereas it depresses excitability of cardiac tissues [75, 84], correlating to neurotoxic [85, 89] and cardioprotective [16, 76-79] effects, respectively. Therefore, exactly how H_2S is affecting ion channels that rapidly control membrane excitability, has become a central question. In the cardiovascular system for example, H_2S stimulates the activity of the ATP-sensitive Kir6 (K_{ATP}) channel through the direct sulfhydration of an N-terminal cysteine (C43) residue, hyperpolarizing and dilating blood vessels [75].

The K_{ATP} channel belongs to the Kir family of K^+ channels that establish and regulate the resting membrane potential of cardiomyocytes, smooth muscle cells, pancreatic cells, neurons and various other excitable cells [81]. A wealth of electrophysiological, structural, and biochemical studies has revealed that PIP_2 interacts with Kir channels as a key direct activator [91]. The cysteine residue (C43) implicated in the effect of H_2S on K_{ATP}, happens to be conserved throughout the Kir subfamily and is positioned next to a positively-charged residue critical for coordinating PIP_2 binding to Kir3 channels. Therefore, sulfhydration of this nearby cysteine may be comparable to other post-translational modifications, such as phosphorylation of specific channel residues that directly or allosterically alter channel interactions with PIP_2 [53]. The effect of H_2S on phosphoinositide control of channel activity is thus a critical molecular theme to be clarified. More specifically, we explored the putative effect of H_2S on cytoplasmic cysteine residues of Kir channels (both conserved and distinct).

Here, we demonstrate that the effect of H_2S on Kir channels (Kir2 and Kir3), heterologously expressed in *Xenopus laevis* oocytes, is inhibitory, as opposed to the stimulatory effect on K_{ATP} channels. We used two approaches to study the effects of H_2S on Kir channels by exogenous application of NaHS to Kir2 and Kir3 channels or by overexpressing CSE, the principal enzyme producing H_2S in peripheral tissues. We show that H_2S-mediated inhibition of Kir channels is dependent on the strength of channel-PIP_2 interactions by employing the voltage-clamp technique on whole oocytes as well as the patch clamp technique in excised membrane patches from oocytes. Moreover, we show direct Kir3.2 channel protein sulfhydration using the TSA technique and determine by mutagenesis which cysteine residues are involved in the inhibitory effect of H_2S on this channel. Lastly, using molecular dynamics simulation

experiments we provide mechanistic insight as to how sulfhydration of these specific cysteine residues leads to changes in channel-PIP_2 interactions and channel gating.

Chapter 2. Materials and Methods

2.1. Materials and Reagents

Dioctanoyl (diC8) forms of $PI(4,5)P_2$, were purchased from Echelon (Salt Lake, UT). They were dissolved in water to make 6.0 mM stock solutions, which were divided into aliquots and stored at -80°C. Further dilutions were made in bath solutions on the day of the experiment. LC arachidonyl-stearyl (AASt) $PI(4,5)P_2$ was purchased from Avanti (Alabaster, AL). Aqueous stock and working solutions were prepared and sonicated as described [66, 92]. Sodium hydrosulfide (NaHS) was purchased from Strem(Newburyport, MA) and dissolved in water to make 100 mM stock solutions, which were divided into aliquots and stored at -20°C. Further dilutions were made in incubation solution on the day of the experiment. DL-Propargylglycine (PAG) was purchased from Sigma-Aldrich, was stored at 100 mM stocks, and used at 5 mM working concentrations. Wortmannin was purchased from Tocris (Bristol UK), and dissolved in DMSO from Sigma-Aldrich (St Louis, MO) to a stock concentration of 20 mM, and stored at -80°C and was diluted to a 5 μM working concentration in experiments.

2.2 Molecular Biology

A Cys-less mutant of Kir3.2C [93] was provided by the Slesinger lab (Icahn School of Medicine at Mount Sinai, NY). Because Kir3.2C (425aa) is a longer splice variant with an additional 11aa at the C-terminus, we generated a Cys-less Kir3.2 (414aa) isoform by PCR. The Kir3.2(E152D) (referred to as Kir3.2*) mutation that boosts homomeric currents (Yi et al., 2001) was introduced and the resulting Kir3.2* (Cys-less) channel was subcloned in the oocyte and

mammalian expression vector pXoom, so that it may be compared to the Kir3.2* 2A subtype. Desired point and double point mutations were introduced by the commercial QuikChange (Agilent Technologies) method. All mutations were confirmed by DNA sequencing (Genewiz). CSE constructs in pcDNA3 were cut with BamHI and HindIII and subcloned into the pGEMHE vector, cut at SmaI and HindIII sites.

Xenopus laevis oocyte expression -- All pGEMHE constructs were linearized using the NheI restriction enzyme, whereas pXoom constructs were linearized using the XhoI restriction enzyme and *in vitro*–transcribed using the mMessage mMachine® Kit (Ambion) kit. Complementary RNA (cRNA) concentrations were quantified by optical density. *Xenopus* oocytes were surgically extracted, dissociated and defolliculated by collagenase treatment, and microinjected with 50 nl of a water solution containing the desired cRNAs. All constructs used in this study were injected to achieve between 5-20 ng per oocyte, depending on the channel and co-injection of CSE, CiVSP or PIP5-Kinase (PIP5K) cRNA. Oocytes were incubated for 2 to 4 days at 18°C.

2.3 Electrophysiology

Whole oocyte currents were measured by conventional Two-electrode voltage clamp (TEVC) with a GeneClamp 500 (Axon Instruments) or TEC-03X (NPI) amplifiers. Currents were acquired at 10kHz and filtered at 2 kHz using NPI software. Agarose cushion microelectrodes were filled with 1.5% (w/v) agarose in 3 M KCl and were used with resistances between 0.1 and 1.0 MΩ. Oocytes were held at 0 mV, and currents were assessed by 800-ms ramps from −80 to +80 mV (at ramp speed of 200 mV/s). Currents at −80 mV were recorded. Barium-sensitive basal currents were defined as the difference between the steady-state currents while perfusing a high-potassium (ND96K or HK) solution or a barium solution. The HK

solution contained the following: 96 mM KCl, 1 mM NaCl, 1 mM $MgCl_2$, 5 mM KOH/Hepes (pH 7.4). The Barium solution consisted of HK + 3 mM $BaCl_2$. Five to twenty oocytes from the same batch were recorded for each group, and the experiments were repeated in at least two batches. A specialized voltage protocol was designed to activate Ci-VSP submaximally when they were co-injected in several experiments, whereby Ci-VSP was activated at +10 mV and current levels were monitored by brief pulses to -80 mV. Recovery was analyzed by holding at -80 mV following a one minute +80 mV depolarization protocol that fully inhibited channel current (Fig 7). Data acquisition and analysis were carried out using pClamp9 (Molecular Devices) and OriginPro (Microcal) software.

2.4 NaHS Treatment in TEVC Experiments

Channels were expressed in *Xenopus laevis* oocytes. After ~72 hours of expression, the vehicle group of injected oocytes was transferred to a petri dish containing 2 mM NaCl added to ND96K (High K) solution, whereas the +NaHS group was transferred to a petri dish containing 2 mM NaHS added to ND96K, sealed with Para film and left to incubate for 100 minutes prior to recording (Fig 6). Barium-sensitive basal currents from both groups 1) Vehicle and 2) + NaHS in the presence of High K^+ (HK or ND96K) solution were assessed at -80 mV using Two-electrode voltage clamp. Barium-sensitive currents were normalized to average basal current of vehicle. All experiments were tested in at least 2 batches.

2.5 Wortmannin Treatment and Recording in TEVC Experiments

Channels were expressed in *Xenopus laevis* oocytes. After ~72 hours of expression, the vehicle group of injected oocytes was transferred to a petri dish containing 2 mL of ND96K and 5 µL Dimethyl sulfoxide (DMSO). The +Wort group of injected oocytes was transferred to a petri dish containing 2 mL of ND96K and 5 µL 10 mM stock solution of Wort (in DMSO).

Figure 6. NaHS Incubation Methodology. Channels were expressed in *Xenopus laevis* oocytes. After ~72 hours of expression, the **Vehicle** group of injected oocytes was transferred to a petri dish containing 2 mM NaCl (and recorded subsequently), whereas the **+NaHS** group was transferred to a petri dish containing 2 mM NaHS, sealed with Para film and left to incubate for 100 minutes prior to recording. Barium-sensitive basal currents from both groups **1) Vehicle** and **2) + NaHS** in the presence of High K^+ (HK or ND96K) solution were assessed at -80 mV using Two-electrode voltage clamp. Barium-sensitive currents were normalized to average basal current of vehicle (2 oocyte group.

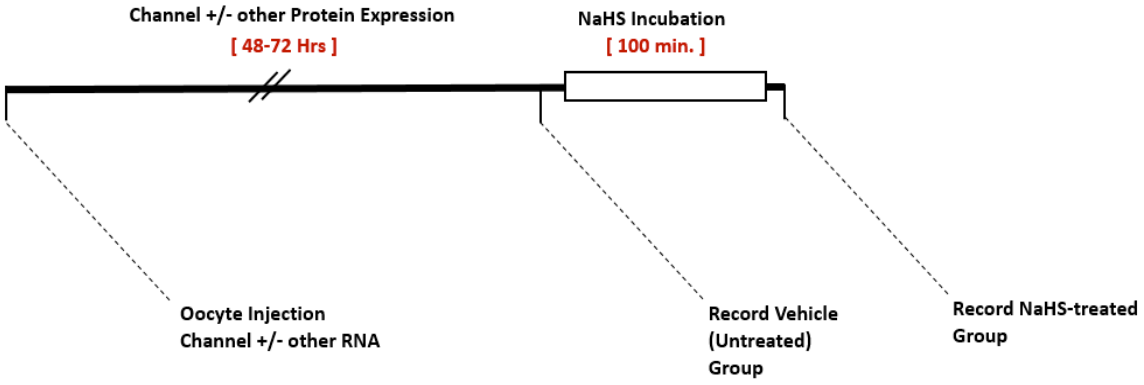
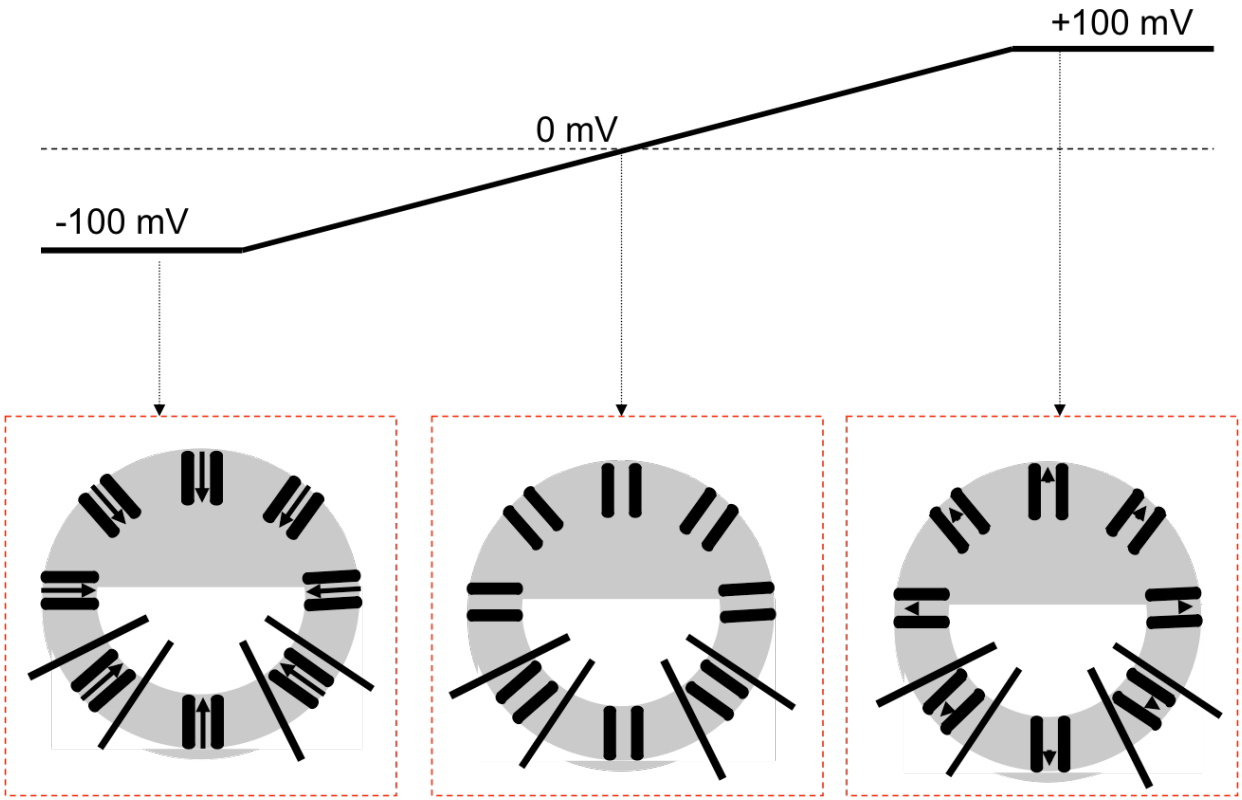


Figure 7. A schematic demonstrating inwardly-rectifying whole-cell potassium currents in *Xenopus laevis* oocytes using the ramp protocol. When a voltage ramp protocol from -100 mV to +100 mV (ramp speed of 200 mV/s) is applied to the oocyte membrane, it changes the electrical driving force across the membrane, rapidly altering the membrane potential linearly. The length and direction of the arrows correspond to net K^+ ion movement and direction of movement across the oocyte membrane. Concentration of K^+ ions are assumed to be equal across the membrane (roughly 90 mM), contributing to 0 chemical driving force across the membrane. **Top.** Voltage ramp protocol applied to the oocyte. **Bottom-left:** Schematic shows robust net inward current corresponding to hyperpolarizing voltage of the ramp protocol (-100 mV), held for 100 ms. **Bottom-middle:** Schematic shows no net movement of K^+ ions (at 0 mV, absence of electrical driving force). **Bottom-right:** Schematic shows significantly less net outward movement of K^+ ions regardless of application of symmetric depolarizing current (+100 mV), held for 100 ms, across the membrane.



Oocytes (5-10) from vehicle and +Wort groups were then assayed as described above in "Electrophysiology" (TEVC) methods, 120 minutes following incubation. Oocytes from the +Wort dish were then transferred to solution containing same solution as the vehicle group (+ 5 µL DMSO in ND96K). Subsequently NaHS was added to both groups for 100 minutes at 2 mM working concentration (as described) and assayed through TEVC recordings.

2.6. Inside-out Macropatch Experiments

The vitelline membrane was manually peeled using forceps to gain access to the oocyte plasma membrane. Pipettes were pulled using a Flaming-Brown micropipette puller and then fire-polished to give a final resistance of 0.8 to 1.2 MΩs. Currents were acquired at 10 kHz and filtered at 2 kHz using pClamp software and the Axopatch 200A amplifier (Axon Instruments). Inward currents were monitored using a ramp protocol from -100 mV to +100 mV, with the holding potential at 0 mV. Following gigaseal formation, the pipette was pulled away from the membrane to achieve an inside-out patch, and perfused directly using a multi-barrel gravity-driven perfusion apparatus. Pipette solution contained (in mM): 96 KCl, 10 HEPES, 1.8 CaCl2, 1 $MgCl_2$, 1 NaCl, pH 7.4. Bath solution (in mM): 76 KCl, 20 NaCl, 5 EGTA, 10 HEPES, pH 7.4.

2.7. NaHS Treatment in Macropatch Experiments

NaHS dose-response curve (dic8 PIP_2). Once the inside-out patch (technique described above) expressing Kir2.3 channels was isolated and once the channel activity ran down, the patch was subjected to 25 µM dic8 PIP_2 until the current reached a steady state, after which, the patch was subjected to NaHS treatment in pipette solution for 200 seconds and reactivated by diC8 PIP_2. Subsequently, the patch was subjected to various concentrations of NaHS for a 200

second duration and currents produced by subsequent 25 μM dic8 PIP_2 pulses were recorded and compared. NaHS dose-response curve (LC-PIP_2). We used the same technique as we did to generate the NaHS dose response curve pulsed by 25 μM diC8 PIP_2, but now we applied ~10 μM solubilized long-chain PIP_2 until currents reached steady-state and then we subjected them to varying concentrations of NaHS following 200 second intervals. Dic8 PIP_2 dose-response curve. Inside out patches expressing Kir2.3 channels were allowed to run down and pulsed by varying diC8 PIP_2 concentrations, then the same patch was exposed to 100 μM NaHS for 200 seconds, and pulsed by the same range of diC8 PIP_2 concentrations.

2.8. TAG Switch Assay

Presence of sufhydration was determined with a recently designed modified tag switch assay [37] by Tyler Hendon (Virginia Commonwealth University), using reagents developed by Sumanta Garai and Ganesh Thakur from Northeastern University. First, Kir3.2* was expressed and purified from Pichia pastoris by Dr. Takeharu Kawano as described previously [54]. Then, approximately 0.6μg/μl of protein was exposed to 1 mM NaHS for 16 min at room temperature to trigger sulfhydration of cysteine residues. Next, 10 mM methysulfonyl benzothiazole (MSBT) exposure for 15 min at room temperature was used to form R-S-BT and R-S-S-BT adducts at the R-SH and R-S-SH moieties of the cysteines, respectively. Excess MSBT was removed by Micro Bio-Spin P-6 Gel Columns. A combination nucleophile and reporter molecule, CN-biotin, was employed at 2 mM for 1 hour at room temperature in a reaction that is highly preferential to R-S-S-BT over all other moieties – resulting in a biotin tag detectible on sulfhydrated cysteines only. Excess CN-biotin was removed by Micro Bio-Spin P-6 Gel Columns. Next, streptavidin-agarose beads were used for 1 hour at room temperature to precipitate biotinylated proteins, followed by detection via Western blot using anti-GIRK antibodies. Preparation of 2-

(methylsulfonyl)benzo[d]thiazole [MSBT]. Periodic acid (1.3 g, 5.80 mmol) was dissolved in CH_3CN (15 mL) by vigorous stirring at room temperature for 1 h. Then CrO_3 (27.5 mg, 0.27 mmol, 10 mol %) was added to the solution. The mixture was stirred at room temperature for 5 min to give a clear orange solution. The H_5IO_6/CrO_3 solution was then added dropwise over a period of 45 min to a solution of 2-(methylthio)benzo[d]thiazole (0.5 gm, 2.76 mmol) in ethyl acetate (30 mL) at 0 °C. After the addition was completed, the reaction mixture was stirred at room temperature for 12 h. The reaction was quenched by addition of saturated Na_2SO_3 solution (2 mL) and filtered, and the solids were washed with ethyl acetate (60 mL). The filtrate was washed, respectively, with saturated aqueous Na_2SO_3 solution and brine and then dried over anhydrous Na_2SO_4. The solvent was evaporated under reduced pressure. The crude reaction mixture was purified by flash chromatography (hexane/ethyl acetate) to obtain MSBT (0.470 gm, 82%) as a white solid. ^{1}H NMR (500 MHz, $CDCl_3$): δ 8.22 (d, J=8.3 Hz, 1H), 8.03 (d, J=8.0 Hz, 1H), 7.63-7.59 (m, 2H), 3.42 (s, 3H); MS-ESI (m/z): 214 $[M+H]^+$. Preparation of 2-(5-((3aS,4S,6aR)-2-oxohexahydro-1H-thieno[3,4-d]imidazol-4-yl)pentanamido)ethyl 2-cyanoacetate (CN-biotin). This compound was synthesized by following a literature reported procedure [37] and the spectral data were matched with the reported compound.

2.9. Molecular Dynamics Experiments

Dr. Yu Xu (Northeastern University) conducted Molecular Dynamics (MD) experiments reported in this thesis. The Kir3.2* control channel or the sulfhydrated Kir3.2* (added –SH to C65, C221-negative control, or C321) channel with 4 PIP_2 molecules were subjected to MD simulations, in which GROMACS v4.5 was used to conduct the simulation, applying the GROMOS96 53a6 force field. The topology files and charges for the PIP_2 atoms were calculated

using the PRODRG web-server, as described in previous work. Meanwhile, the topology file of the sulfhydrated-Cys residue was generated based on existing force field parameters. The channel-PIP_2 structures were immersed in an explicit POPC bilayer using the VMD membrane package, and solvated with SPC water molecules with 150 mM KCl. To mimic the activated state, we applied a constant depolarizing electric field of -0.128 $mV \cdot nm^{-1}$. Energy minimization was performed, followed by a 300ps position-restrained (1000 $kJ/mol/nm^2$) MD run. Subsequently, the four systems were subjected to a 25 ns MD simulation. Analysis: The SIMULAID program was used to analyze/cluster structures, and to calculate interaction networks, including hydrogen bonds, salt bridges and hydrophobic contacts.

3.0. Statistics

Data are reported as mean ± SEM; n denotes the number of oocytes. Unpaired (two sample) t-tests were performed in most statistical analysis of TEVC experiments, and normalized currents from oocyte group exposed to NaHS were compared to that of the vehicle (untreated) group with an overall significance level of $P < 0.05$ using OriginPro 2016 (Microcal). Currents were normalized to the average current of vehicle (untreated) group. To determine whether there are significant changes upon exposing oocyte groups to NaHS at increasing time periods, as well as increasing RNA injection amounts of CSE, one-way repeated-measures ANOVA were performed, and pairwise comparisons were made by the Holm-Sidak method with an overall significance level of $P < 0.05$ in OriginPro 2016 (Microcal). Inhibition (±SEM) of currents by NaHS in inside-out (I/O) macropatches was normalized to current elicited by PIP_2 (prior to NaHS treatment), and non-linear fitting of current inhibition was done in OriginPro 2016 using the Growth/Sigmoidal category, DoseRep function and Levenberg Marquardt iteration function to the following equation:

$$y = A1 + \frac{A2 - A1}{1 + 10^{(LOGx0 - x)p}}$$

in which, y is the normalized current, x is the concentration of NaHS or diC8 applied to patch, A1 is minimum value, A2 is the maximum value, and p is the parameter for the variable hill slope.

Chapter 3. Hydrogen Sulfide Regulation of Kir Channel Activity is PIP_2-dependent and Mediated by Specific Cysteine Residues

3.1. Dual Role of NaHS on Kir Channels and Sulfhydration of Kir3.2 Channels

In contrast to previous studies on stimulation of vascular K_{ATP} (Kir6.1) channels [75], NaHS (2 mM) treatment inhibited Kir3.2* channel activity (* indicates the E152D mutant that increases homomeric channel activity) [94]. NaHS administration to Kir3.2* channels expressed in *Xenopus* oocytes inhibited the whole-cell currents in a time dependent manner, affecting Kir3.2* channels maximally at ~100 minutes, whereas treatment for 400 minutes did not produce an additional effect (Fig. 8A). Therefore, the effect of NaHS was observed and compared when oocyte groups were treated for 100 minutes in successive experiments. In order to explore whether the NaHS effect was direct on the Kir3.2 protein, Tyler Hendon employed the TAG Switch Assay (as described in Materials and Methods) and observed chemical modification of a band corresponding to ~48kDa, which is approximately the expected molecular weight of Kir3.2 (Fig. 8B). Similar to hydrogen sulfide-mediated inhibition of Kir3.2* channels, NaHS treatment diminished currents from oocytes expressing cardiac Kir3.4 channels, both homomeric Kir3.4* (* denotes S143T, a mutant shown to boost Kir3.4 homomeric activity) [95], heteromeric Kir3.4/Kir3.1 channels (Fig. 8C), and Kir2.3 channels, another Kir subfamily member (Fig. 8D).

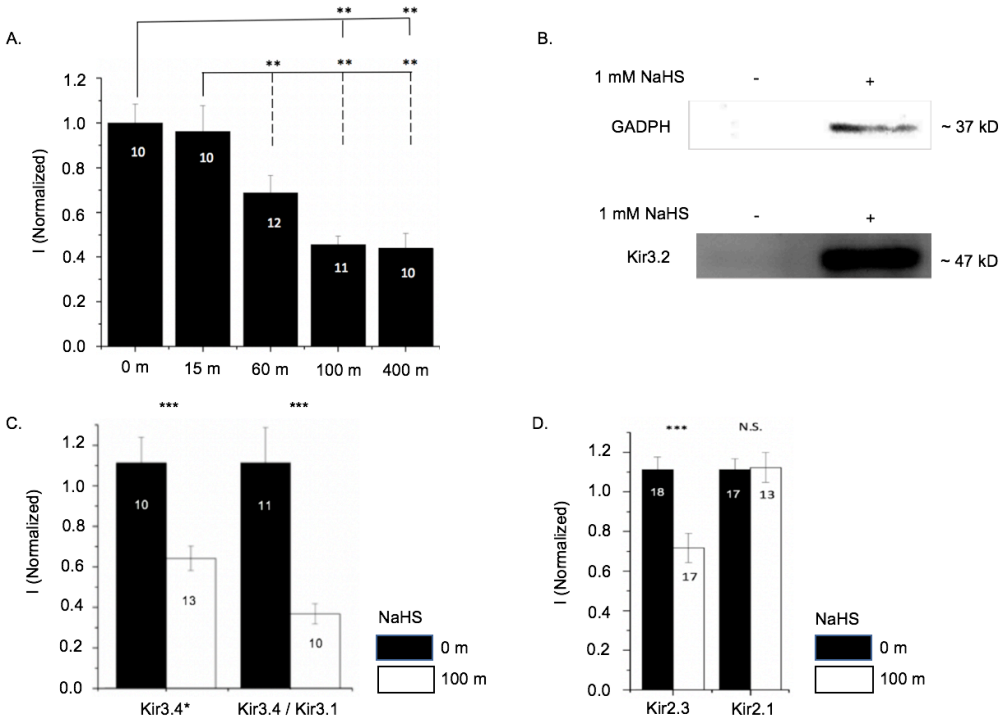
Interestingly, Kir2.1 activity was unaffected by NaHS treatment (Fig. 8D). Conversely, NaHS treatment augmented the activity of the cardiac Kir6.2 channel, consistent with previous experiments on the vascular Kir6.1 channel, when it was either co-expressed with SUR2A subunits or expressed alone as the recombinant Kir6.2Δ36 channel (Fig. 8E) in *Xenopus* oocytes. Kir6.2Δ36 refers to a C-terminal truncation mutant of Kir6.2 that renders these channels active as homomers [96], by removing a 3-aa motif [97] that serves as an endoplasmic reticulum (ER) retention signal.

3.2. NaHS Inhibition of Kir3.2* Channels is Dependent on Channel-PIP_2 Interactions.

A common feature of Kir channels is that they all require the membrane phospholipid phosphatidylinositol (4,5)-bisphosphate (PIP_2) to maintain their activity [67]. The strength of Kir-PIP_2 interactions determines the sensitivity of Kir channels to several regulatory factors such as pH, protein kinase C, and G proteins [54, 69]. Kir2.1 channels, with the highest apparent affinity to PIP_2 among the channels tested, were unaffected by NaHS treatment, suggesting that the extent of NaHS effect may depend on the strength of channel-PIP_2 interactions. To test this hypothesis, we first altered cytoplasmic PIP_2 levels and monitored NaHS-mediated inhibition of Kir3.2* channels. First, NaHS-mediated inhibition of Kir3.2* channels diminished when the intracellular pool of PIP_2 was increased through the co-injection of PIP5 Kinase, a kinase that phosphorylates PIP4, into PI (4,5)P_2 (Fig. 9A). Conversely, depleting intracellular levels of PIP_2 through co-administration of Wortmannin (Wort), a known blocker of PI4-kinases at μM concentrations, permitted greater inhibition of Kir3.2* currents by NaHS (Fig. 9A). Furthermore, the NaHS-mediated inhibition was enhanced by Ci-VSP (voltage activated PIP5 phosphatase) dependent inhibition of Kir3.2* channels (Fig. 9B), another approach used to deplete the intracellular pool of PIP_2. Consistent with these results, bolstering Kir3.2*-PIP_2 interactions

alternatively by co-expressing the G-protein subunit, Gβγ, also attenuated NaHS inhibition of Kir3.2* current (Fig. 9C). Then we tested what would happen to the extent of NaHS-mediated inhibition when Kir3.2 channels themselves were altered intrinsically using known point mutations that increase channel-PIP_2 interactions. For example, the E152D point mutation in Kir3.2* was shown previously to strengthen channel-PIP_2 interactions [54], and thus it was not surprising to see that NaHS had a greater inhibitory effect on wild-type Kir3.2 homomeric channels with a weaker apparent PIP_2 affinity than Kir3.2* channels. Moreover, the inhibitory effect of NaHS was virtually abolished when the point mutation (I234L) in the background of Kir3.2* channels that further strengthens the apparent channel-PIP_2 affinity (Fig. 9D).

Figure 8. Exogenous H_2S Inhibits Kir3.x and Kir 2.x Channels and Activates Kir6.2 Channels. NaHS-treated currents are normalized to vehicle (untreated) group. A. H_2S inhibits Kir3.2* (E152D) homomeric channel activity. Incubation of Kir3.2* channels with 2mM NaHS elicits time-dependent inhibition. Treatment with NaHS at increasing intervals leads to following normalized current values: 1.01 +/- 0.14 (15 min), 0.72 +/- 0.05 (60 min), 0.54 +/- 0.04 (100 min), and 0.55 +/-0.05 (400 min). Post-incubation, Kir3.2* activity is maximally inhibited by ~45% at 100 minutes (and not further inhibited at 400 minutes). B. Tag Switch Assay detects sulfhydration of purified Kir3.2 channels treated with NaHS. Left Panel: The exogenous application of NaHS (1mM) to GADPH from HEK cell lysates yields a band at ~37 k. Right Panel: Exogenous application of NaHS (1mM) to purified Kir3.2 protein leads to detection of direct sulfhydration of channel (~47 kDa band). C. H_2S inhibits cardiac Kir3.4 (S143T) homomeric channel and Kir3.4/Kir3.1heteromeric channel activity. Treatment with NaHS led ~55% inhibition of Kir3.4* channels (0.45 +/-0.02) and ~61% inhibition of Kir3.4/Kir3.1 channels (0.39 +/- 0.02). D. H_2S inhibits Kir2.3 channel activity but has no effect on Kir2.1 channel activity. Treatment with NaHS significantly inhibited Kir2.3 channels (0.74 +/-0.06) but did not significantly alter Kir2.1 channel activity (1.04 +/- 0.11). E. Currents from both groups of oocytes expressing Kir6.2/SUR2A or Kir6.2Delta36, in which the terminal 36 C-terminal amino acids are removed from Kir6.2 to permit cell surface expression in the absence of Sulfonylurea receptor (SUR2A) subunits, increased approximately 8-fold (normalized current values of 8.49 +/- 2.46 and 8.01 +/- 0.73 respectively) upon incubation with 2 mM NaHS, consistent with hyperpolarizing findings in Mustafa et. al. (2011), in which Kir6.1 was expressed in HEK293 cells. * indicates comparison to the untreated group. Single, double, and triple symbols indicate $p < 0.05$, $p < 0.01$, and $p < 0.001$, respectively.



3.3. Micromolar Concentrations of NaHS Inhibit Kir2.3 Channels in Macropatch Recordings

NaHS incubation of whole oocytes expressing Kir channels led to significant inhibition of various Kir2.x and Kir3.x channel activities, whereas it stimulated Kir6.2 activity. We proceeded to apply NaHS to the cytoplasmic side of excised inside-out patches expressing Kir channels to examine directly H_2S effects, isolating the channel and other membrane-delimited elements from the rest of the cellular cytoplasm. We used Kir2.3, whose relative phosphoinositide-interaction profile has been characterized as moderate in previous experiments, thus yielding reasonable currents in excised patches. Kir2.3 was inhibited by NaHS in TEVC recordings (Fig. 8D). First, we tested the effect of applying NaHS at the micromolar range of concentrations and chose to use a single (sub-maximal) concentration of soluble PIP_2, diC8 (25 μM), to compare the relative NaHS effects. Not surprisingly, Kir2.3 channel activity was inhibited (Fig. 10A) by NaHS in a dose-dependent manner (IC_{50} ~ 83 μM), and channel activity was maximally inhibited by ~64%, similar to the inhibition measured in whole oocytes incubated with NaHS (Fig. 8D). Interestingly, NaHS also elicited dose-dependent inhibition of Kir2.3 when the channels were maximally activated with long chain PIP_2, (Fig. 10B), but showed a lesser extent of inhibition (~37% maximal inhibition) than when Kir2.3 channels were activated by 25 μM diC8 PIP_2 (Fig. 10A), consistent with the decrease of NaHS effects when channel-PIP_2 interactions are strengthened, as seen in the whole oocyte experiments (Fig. 9). Conversely, we performed dose-response measurements of PIP_2 before and after inhibition by NaHS (100 μM, close to IC_{50} in Fig. 10A) to examine how NaHS treatment might affect channel-PIP_2 interactions. We determined that NaHS treatment to the patch (Fig. 10C and D) right shifted the PIP_2 dose-response curve, decreasing the apparent affinity of PIP_2 demonstrated by the increase

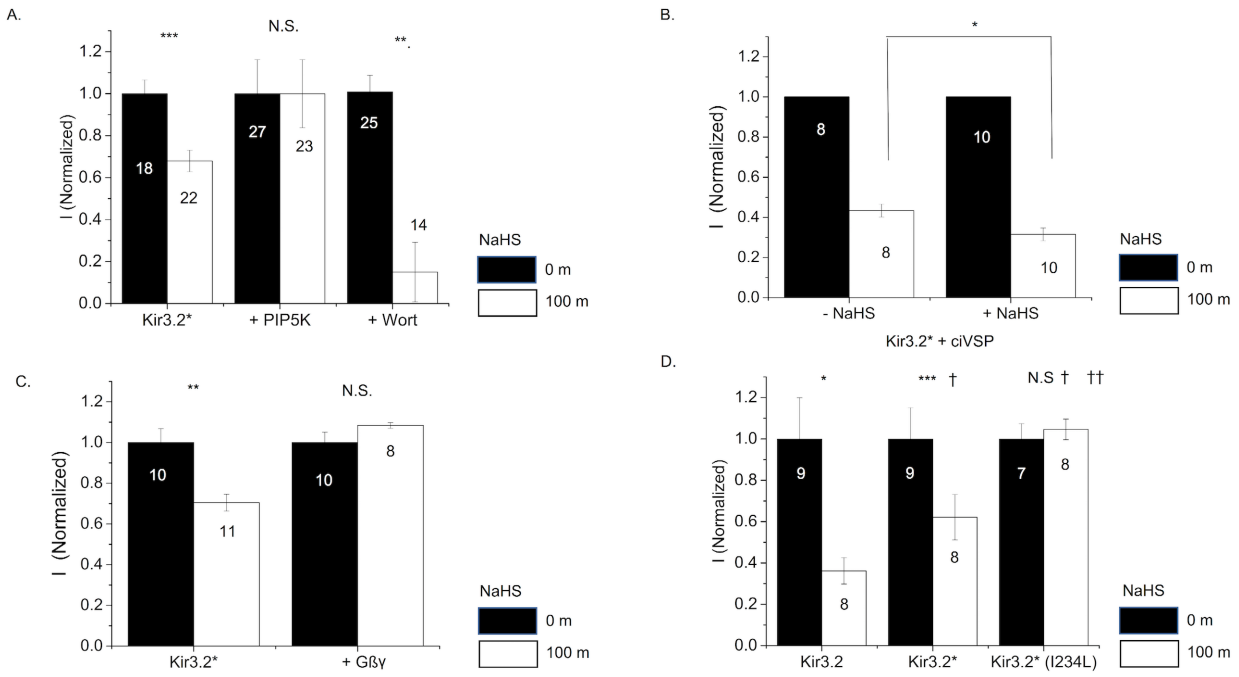
of EC_{50} from 6.2 μM to 9.6 μM. Interestingly, direct NaHS treatment dramatically reduced the potency of PIP_2, indicated by ~29% reduction in maximal activity following NaHS treatment.

3.4. NaHS Inhibition of Kir3.2* Channels is Mediated by Sulfhydration of Specific Cytoplasmic Cysteine Residues

Hydrogen Sulfide (H_2S) is a gasotransmitter that has been shown to signal via sulfhydration, a post-translational modification of reactive cysteine residues and conversion of the Cys –SH group to an –SSH group. It was previously shown that NaHS is able to sulfhydrate a specific cysteine residue, of vascular K_{ATP} channels (Kir6.1), leading to eventual hyperpolarization and vasodilation of superior mesenteric arteries, and its substitution with serine (C43S) abolished the NaHS effects [75]. This specific cysteine residue is conserved throughout Kir subfamily members, and positioned adjacent to a positively charged cytoplasmic residue shown in the Kir3.2 crystal structure to interact electrostatically with one of the negatively charged phosphate groups of PIP_2, critical for channel gating [98].

In the cytoplasmic region of the Kir3.2 channel, there are three putative cysteine residues C190, C221, and C321 that may be sulfhydrated in addition to C65, the conserved cysteine residue corresponding to C43 in Kir6.1 channels (Fig. 11A, top panel). In addition to the four cytoplasmic cysteine residues, Kir3.2 channels also have two extracellular cysteine residues, C134 and C166, located in the extracellular loop region (ECL) and involved in intersubunit disulfide interactions.

Figure 9. Hydrogen Sulfide Inhibition of Kir3.2 Channels is Altered by Strengthening or Weakening Channel-PIP_2 Interactions. A. Increasing PIP_2 concentration in the oocyte (and thereby increasing channel-PIP_2 interactions) through the co-expression of PIP5 Kinase (PIP5K) virtually abrogates H_2S inhibition of Kir3.2* channels, whereas reduction of PIP_2 levels via oocyte incubation in 25 μM Wortmannin (Wort, known blocker of PI4-kinases at μM concentrations and PI3-kinases at nM concentrations) for 100 minutes in untreated oocytes or co-incubation (with NaHS), enhanced H_2S inhibition from ~40% to ~80% inhibition. B. Decreasing PIP_2 though activation of co-expressed Ci-VSP, a voltage activated PIP5 phosphatase, also reduces intracellular PIP_2 and H_2S is able to enhance channel inhibition (~70% inhibition compared to ~60% inhibition for untreated oocytes). C. Co-expression with Gβγ another allosteric enhancer of Kir3.2-PIP_2 interactions, also reduced the NaHS inhibitory effect on Kir3.2* channels (from NaHS treated value of 0.66 +/- 0.05 to 1.08 +/- 0.01). D. H_2S effect on Kir3.2 weakens when channel-PIP_2 interactions are strengthened through point mutations. Whereas Kir3.2 (WT) channel is greatly inhibited by NaHS treatment (0.36 +/- 0.06), pore point mutation (E152D) in the background of Kir3.2 strengthens channel-PIP_2 interaction and diminishes Kir3.2 inhibition by H_2S (0.62 +/-0.11). Additional point mutation (I234L), in the background of the Kir3.2* (E152D) mutation, further strengthens channel-PIP_2, completely abrogating the H_2S inhibition (1.04 +/- 0.11). *indicates comparison to untreated group. Double and triple symbols $p< 0.01$, and $p < 0.001$ respectively.

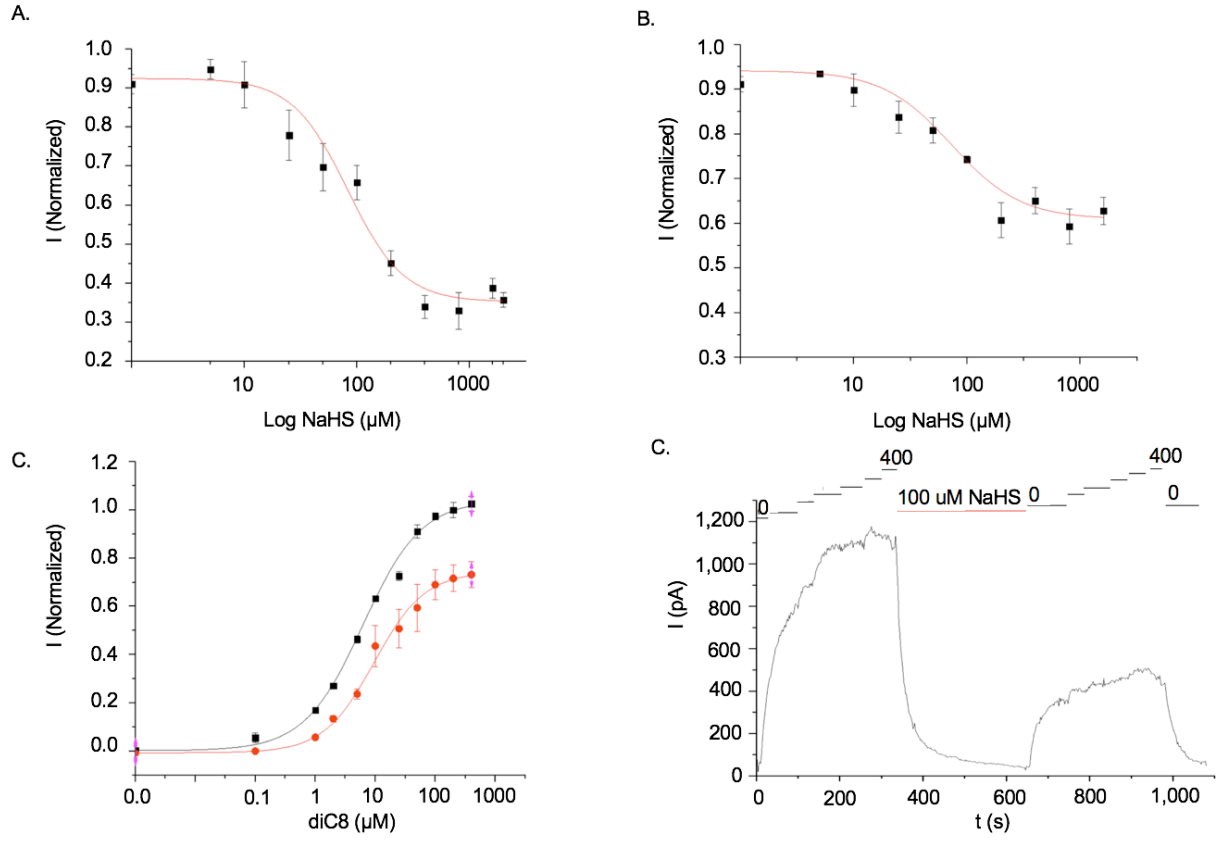


A functional Kir3.2* 'Cys-less' mutant lacking all four cytoplasmic cysteine residues (scheme in Fig. 11A, bottom panel) characterized in previous experiments [93] was refractory to NaHS inhibition (0% inhibition), and NaHS effect (~37% inhibition) was partially restored by reintroducing individual cysteines to the Kir3.2* Cys-less mutants at positions 65 (~18% inhibition) or 321(~25% inhibition), and the NaHS effect on Kir3.2* was fully restored through reintroduction of both specific cysteines, 65 and 321 (Fig. 11B). Kir3.2* Cys-less mutant channels also showed no significant differences in apparent PIP_2 affinity compared to Kir3.2* channels when tested by the voltage-gated lipid phosphatase Ci-VSP (Fig. 12). More specifically, Kir3.2* showed no difference in rate of inhibition compared to Kir3.2* Cys-less (2.3s $tau_{Inhibition}$ for Kir3.2* and Kir3.2* Cys-less) and no change in recovery rates while possessing faster inhibition (compared to $tau_{Inhibition}$ of 11.5s) and faster recovery kinetics than Kir3.2*(I234L), a channel shown previously to have increased channel-PIP_2 interactions (Fig 12).

3.5. Cystathionine γ-lyase (CSE) Co-expression Mimics Exogenous NaHS Effects on Kir3.2* Channels

Cystathionine γ-lyase (CSE), is an enzyme central to the production of H_2S in cardiac tissue and specific regions of the brain (hippocampus and striatal neurons) in physiological and pathophysiological conditions [7, 14] and therefore, most likely to be co-expressed in neurons with Kir3.2 channels and Kir2.x channels (as well as Kir3.4 channels in cardiac cells). Among the three enzymes that produce H_2S, CSE seems to be the most inducible and is modulated in diverse conditions such as inflammation mediated by tumor necrosis factor (TNF) and lipopolysaccharides (LPS), metabolites such as glucocorticoids and glucose, as well as dietary restriction and endoplasmic reticulum (ER) stress thereby making it an attractive therapeutic

Figure 10. H_2S Inhibition of Kir2.3 Channels is Mediated by Micromolar Concentrations of NaHS in Macropatches. A. H_2S inhibits Kir2.3 channel activity in macropatches activated submaximally by soluble PIP_2 (25 μM diC8). Direct administration of varying concentrations of NaHS to the cytoplasmic surface of inside-out patches expressing Kir2.3 channels leads to concentration-dependent inhibition of Kir2.3 channel activity (IC_{50} = 82.95 +/-15.47 μM and A1 value = 0.36 +/- 0.02) when they are pulsed (activated) by 25 μM soluble dioctanoyl PIP_2 (diC8). B. H_2S also inhibits Kir2.3 channel activity in macropatches maximally activated by LC-PIP_2 (full-length PIP_2), but to a lesser extent than 25 μM diC8 pulses (Fig. 3A). Direct administration of varying NaHS concentrations to the cytoplasmic surface of inside-out patches expressing Kir2.3 channels led to concentration-dependent inhibition of Kir2.3 channel activity (IC_{50} = 73.21 +/-12.50 μM and A1 value = 0.71 +/- 0.03) when they are activated by full length PIP_2. C. H_2S (100 μM NaHS) reduces the efficacy (increased EC_{50} values from 6.20 +/-0.50 μM to 9.60 +/-1.17 μM) and potency (A2 value decreases from 1.04 +/- 0.04 to 0.74 +/-0.03) of Kir2.3 channel activation by soluble PIP_2 (diC8). D. Representative trace (summarized in Fig. 3C) of Kir2.3 expressing inside-out patches subject to various diC8 PIP_2 concentrations (0 μM, 10 μM, 25 μM, 50 μM, 100, μM, 200 μM, and 400 μM) prior to and after exposure to NaHS (100 μM) for 200 seconds.



target [7, 14]. Co-expression of CSE with Kir3.2* in *Xenopus* oocytes recapitulated the inhibition of Kir3.2* produced by exogenously applied H_2S (NaHS), in which increasing the cRNA amount co-injected (ranging from 0.5 – 8.0 ng) resulted in a dose-dependent inhibition of Kir3.2* currents (Fig. 13A). The Cys-less Kir3.2* channel, refractory to exogenous NaHS treatment, was also unaffected by CSE co-expression (Fig. 13B). Acute treatment with 5mM propargylglycine (PAG) for 100 minutes, an inhibitor of CSE activity, reversed CSE inhibition of Kir3.2*, whereas it did not affect significantly Kir3.2* channels expressed alone (Fig. 13C).

3.6. Molecular Dynamics Experiments Show Sulfhydration of Specific Cysteine Residues Alters Channel Gating and Interactions with PIP_2

In order to gain a better mechanistic understanding about how sulfhydration of a specific cysteine residue (the functional effects demonstrated experimentally in Fig. 11B) may affect channel-PIP_2 interactions as well as channel gating, Dr. Yu Xu performed molecular dynamics (MD) simulations with Kir3.2 co-crystallized with PIP_2 (PDB code 3SYQ) to model the sulfhydration-induced Kir channel inhibition [98, 99]. More specifically, we induced sulfhydration of three cysteine residues, C65, C321 (positive effects in Fig. 11B) or C221 (no effect in Fig. 11B) and performed a 25ns MD simulation run to observe whether dynamic changes occurred to a) the G-loop gate, integral for Kir3.2 channel gating and b) the channel-PIP_2 interactions. First, we surveyed the minimal distances between one of the two phosphates on the PIP_2 inositol ring and the Lysine residue, K64, previously characterized as critical for Kir3.2-PIP_2 channel interactions [98] and observed an increase in the distances when C65 (Red) or C321 (Gold) residues were sulfhydrated but not when C221 (Green) was sulfhydrated (Fig. 14A). Dashed lines in the model snapshots taken from the molecular dynamics experiment detail how K64 residue moved away from the phosphate on the PIP_2 head group when C65 or C321

was sulfhydrated (Fig. 14B). Consistent with these observations, scoring the average channel-PIP_2 channel interactions (the limit was specified as being within 0.7 nm), revealed that sulfhydration of C65 or C321 (and not C221) residues decreased interactions between the PIP_2 and the channel (Table 1). Dr. Yu Xu then sought to determine whether sulfhydration affects channel gating and monitored the minimal distance of the G-loop gate between the alpha carbons of T317 on opposite Kir3.2 subunits. We observed a substantial decrease when the C65 or C321 (but not the C221) residue was sulfhydrated, suggestive of constriction of the G-loop gate closure, whereas a minimal change was observed when C221 was sulfhydrated (Fig. 14C). The change in G-loop gate conformation is highlighted by model snapshots (Fig. 14D) of the T317 alpha carbon moving from no sulfhydration (Grey) to C65 (Red), C221 (Green), or C321 (Yellow). In stark contrast, we observed an increase in channel-PIP_2 interactions when a homology model of Kir6.2, based on the Kir3.2 structure (PDB code 3SY), was subjected to sulfhydration at C42 (homologous to C65 in Kir3.2) (bottom panel, Table 1). The sulfhydration of the C42 also led to increases in distance between the analogous alpha carbons (T294) in an MD simulation, suggesting that the G-loop gate opened (Fig. 15), highlighted by the shift of T294 alpha carbons (red) away from the non-sulfhydrated Kir6.2 (grey) (Fig. 15, Right Panel).

Figure 11. Specific Cysteine Residues are Sulfhydrated in Hydrogen Sulfide Regulation of Kir3.2 Channels. A. Top Panel: Model of sulfhydrated cysteine residues is based on Kir3.2 structure (PDB code 3SYQ). Sulfhydrated groups (sulfhydrated cysteine -SH groups) modelled and mapped on to structure of Kir3.2. Four cytoplasmic cysteines are highlighted: C65, C190, C221, and C321.Two extracellular cysteine residues, C134 and C166, located in the extracellular loop region (ECL) and involved in intersubunit disulfide interactions, were not mutated. Highlights show location of C65, and how sulfhydration (space-filling models) may directly interfere with channel-PIP_2 interactions, whereas, C321, when sulfhydrated may give rise to allosteric modifications at the G-loop directly as well as indirectly affect channel-PIP_2 interactions. Bottom Panel: Scheme of functional Kir3.2* Cys-less mutant previously characterized as having intact basal current, response to agonist-induced current [93]. The four cytoplasmic cysteine residues mapped in (A) are mutated to the following residues (from N-terminus to C-terminus): C65V, C190T, C221S, and C321V. B. Kir3.2* Cys-less mutant activity is entirely insensitive to H_2S. NaHS incubation is unable to inhibit Kir3.2*Cys-less mutant (0.985 +/- 0.06). Preliminary data reveal that the strength of Cys-less mutant-PIP_2 interaction is not significantly different from that of Kir3.2*. Re-introducing single cysteine residues to positions 65 and 321 partially restores H_2S inhibition by ~18% (0.82 +/- 0.04) and ~33% (0.67 +/- 0.06) respectively, roughly additive to ~52% inhibition of Kir3.2* (0.58 +/- 0.03) with all four cytoplasmic cysteine residues. Re-introducing single cysteine residues to positions 190 and 221 do not significantly restore H_2S inhibition (0.91 +/- 0.06 and 0.94 +/-0.15 respectively). * indicates comparison to untreated group. Triple symbols (***) indicate $p < 0.001$.

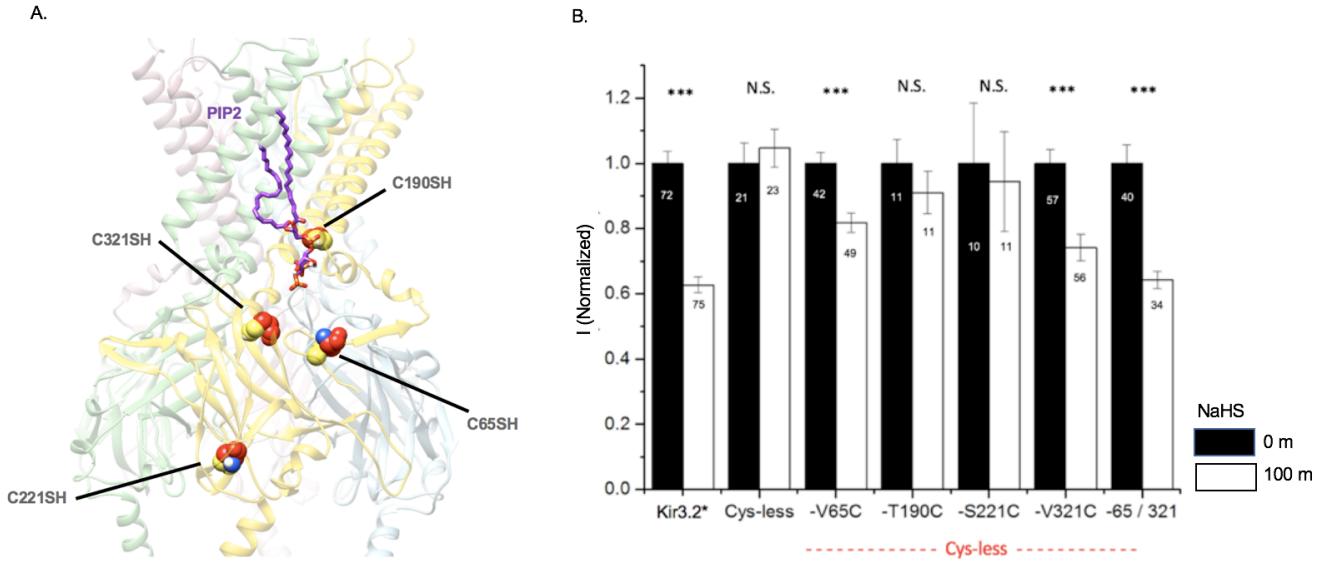


Figure 12. Strength of Channel-PIP_2 interactions are similar between Kir3.2* and Kir3.2* (Cys-less) Channels. A. Voltage protocols (in mV) used for inhibition (top) and recovery (bottom). B. Kir3.2* and Kir3.2* (Cysless) displayed faster current inhibition compared to Kir3.2*(I234L). C. Tau values for inhibition for Kir3.2* of 2.56 +/- 0.06 s and Kir3.2*(Cysless) of 2.78 +/- 0.04 s were not significantly different. However, both tau values were significantly less than that of Kir3.2*(I234L) of 10.1 +/- 0.72s. *** $p<0.001$ compared to control. D. Kir3.2* and Kir3.2* (Cysless) showed slower recovery time than Kir3.2* (I234L) at -80 mV.

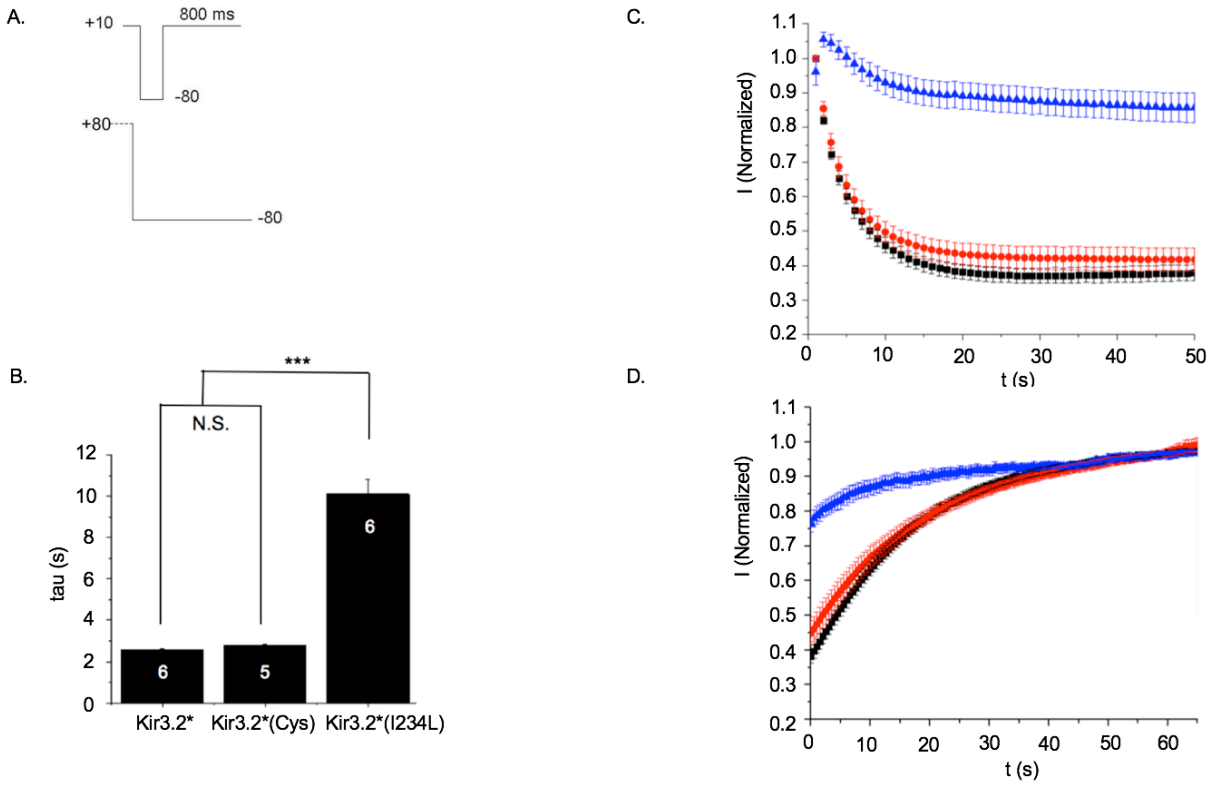


Figure 13. Expression of CSE, Enzymatic Producer of H_2S, Mimics NaHS Effects
A. Co-injection of cystathionine γ-lyase (CSE), integral to the production of H_2S in specific mammalian tissues at physiological concentrations, recapitulates inhibition of Kir3.2* produced by exogenously applied H_2S (NaHS). Increasing CSE mRNA co-injected into oocyte (with Kir3.2* channel), increases significantly Kir3.2* inhibition in a dose-dependent manner, 0.74 +/- 0.05, 0.66 +/- 0.06, and 0.56 +/- 0.06 for 0.5ng, 4.0 ng, and 8.0 ng injections respectively. B. Kir3.2* Cys-less activity is refractory to CSE co-injection. Mutating all four cytoplasmic residues mentioned in Fig. 11A removes the inhibitory effect of co-expressing CSE (1.00 +/- 0.06) compared with that of Kir3.2* WT (0.62 +/- 0.05), strongly suggesting that the reduced Kir3.2* activity is not due to taxing the mRNA machinery in oocytes with a non-specific RNA load. In addition, CSE inhibition requires cytoplasmic cysteine residues as was the case with exogenously applied NaHS. C. Treatment with propargylglycine (PAG), an inhibitor of CSE activity, reversed CSE inhibition of Kir3.2* (from 0.56 +/- 0.11 to 0.90 +/- 0.09). * indicates comparison to only channel injected. † indicates comparison to co-injection with 0.5 ng CSE. Double, and triple symbols indicate $p< 0.01$, and $p < 0.001$ respectively.

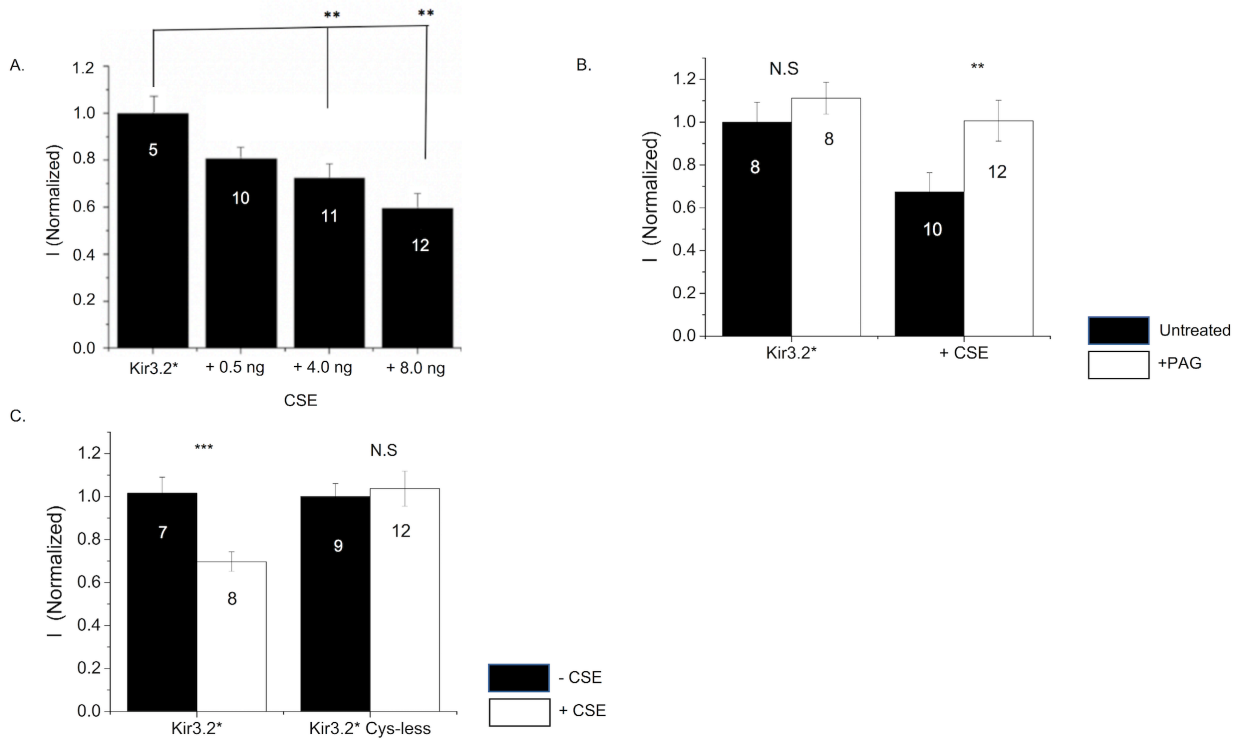


Figure 14. Molecular Dynamics Experiment provides Mechanistic Insight into How Sulfhydration of Specific Residues on Kir3.2 Channels affect channel-PIP_2 Interaction and Channel Gating. MD Simulation (25 ns) reveals how sulfhydration of C65, disrupts direct channel-PIP_2 interactions, between adjacent K64 and PIP_2, consequently leading to closure of the G-loop Gate (decrease in distance between alpha carbons of T317 on opposite subunits). A. Left Panel: MD Simulation subjecting models of Kir3.2* (no cysteine modification) and three of the cysteine-modified, sulfhydrated Kir3.2* channels (C65, C221, and C321) with 4 PIP_2 molecules for 25 ns revealed structure-dynamics-function relationship of a PIP_2 interacting residue, K64 (highlighted in Fig. 11A in the N-terminus region). In this simulation, the distance between K64 and PIP_2 increases in the Kir3.2* model with sulfhydrated C65 or C321 (but not the Kir3.2* models with sulfhydrated C221 or C190 – not shown), suggestive of how H_2S may directly interrupt the K64-PIP_2 interactions. Right Panels: Model snapshots taken from molecular dynamics experiment details how K64 residue (left, no modification) moves away from phosphate on PIP_2 head (distance between residue and PIP_2 (dotted black lines) increases from 8A (no sulfhydration) to 14.9 Å and 10.4 Å for models with C65-SH and C321-SH respectively, whereas no substantial change is detected in the model with C221-SH. B. Left Panel: The G-loop Gate in Kir3.2* closes only when C65 or C321 is sulfhydrated, suggested by the decrease of distance between T317 alpha carbons of opposite subunit G-loops (indicative of closing of G-loop gate when C65 or C321 is sulfhydrated). Right Panels: Alpha carbons of T317 residue move closer (gate closing) from no modification (grey) to when C65 (red) or C321(yellow) is sulfhydrated in MD simulations whereas relatively no change is evident when C221 (green) is sulfhydrated.

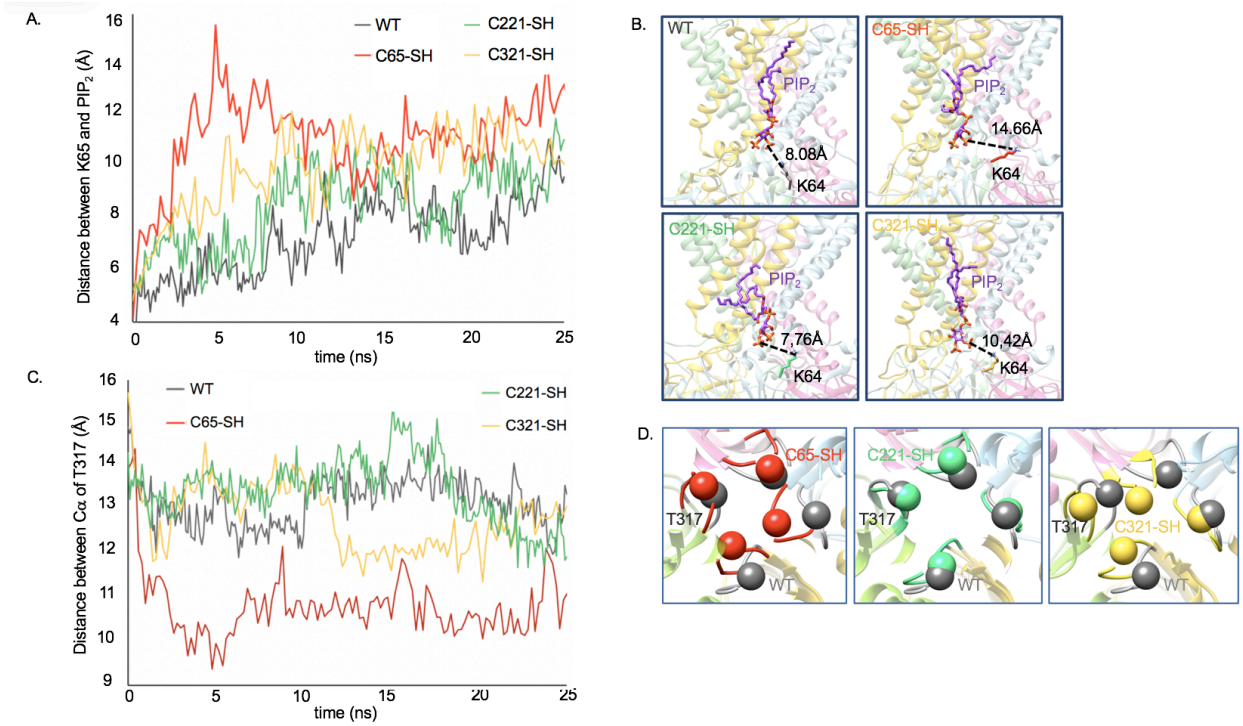


Figure generated by Dr. Yu Xu.
Ha et. al. 2017, In submission to *Journal of Biological Chemistry*

Figure 15. Molecular Dynamics Experiment Provides Mechanistic Insight as to how Sulfhydration of C42 is Permissive Towards Kir6.2 Channel Opening. Left Panel: The G-loop gate in Kir6.2 channel opened when C42 was sulfhydrated, suggested by the increase in the distance between T294 alpha carbons of the G loops of opposite subunits. Right panel: Top view (right) showed how the T294 residue moves away (gate opening) from no modification (grey) to when C42 was sulfhydrated (red).

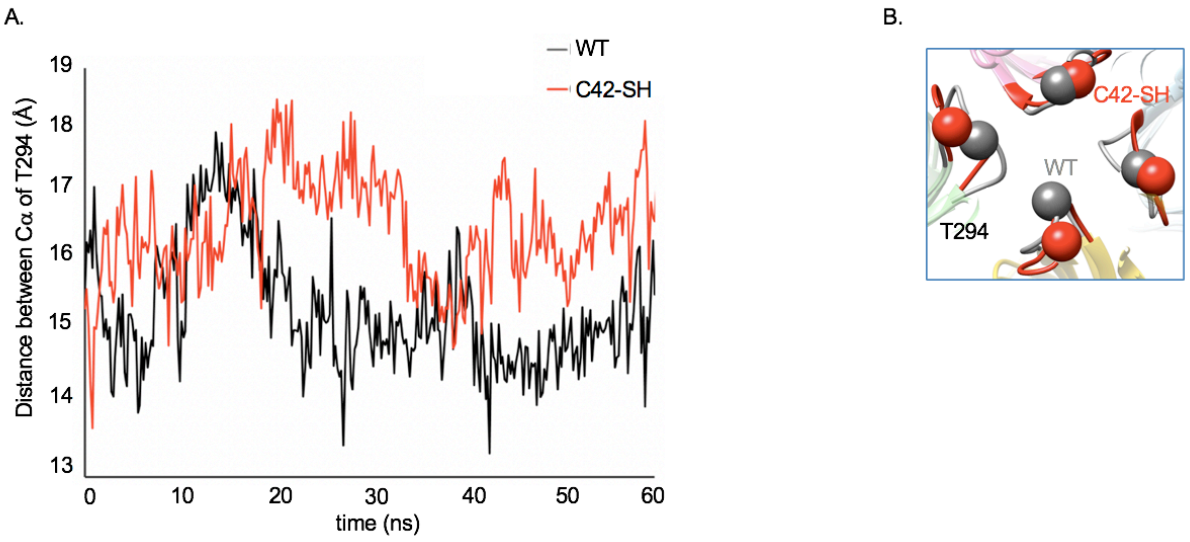


Figure generated by Dr. Yu Xu.
Ha et. al. 2017, In submission to *Journal of Biological Chemistry*

Table 1. Molecular Dynamics Experiment Reveal Direct changes in Channel-PIP_2 Interactions (Total contact between PIP_2 head group and Channels, A.U.)
Top: Kir3.2. Contact frequencies of PIP_2 head groups with channel diminished in MD simulations with sulfhydrated C65 or C321 and not C221, consistent with experimental results. Bottom: Kir6.2. Contact frequencies of PIP_2 head groups with channel increased with sulfhydrated C42, consistent with experimental results.

Total Contacts (A.U.)	No-SH	C65-SH	C221-SH	C321-SH
Kir3.2*	11	7.64	10.3	5.26

Total Contacts (A.U.)	No-SH	C42-SH
Kir6.2	10.9	13.1

Table values produced by Dr. Yu Xu.
Ha et. al. 2017, In submission to *Journal of Biological Chemistry*

Chapter 4. Carbon Monoxide Inhibition of Kir2 and Kir3 Channels is also PIP_2-dependent and mediated by a Specific Cysteine Residue

Carbon monoxide (CO) is produced endogenously by the catabolism of heme by heme oxygenases (analogous to the enzymatic production of hydrogen sulfide by CBS, CSE, or CAT/MST) or exogenously by the partial combustion of hydrocarbon sources. Its physiological actions have also shown to be greatly beneficial to cardiovascular disease, such as the relaxation of vascular smooth muscle involving BK channels. Yet like hydrogen sulfide, in high exogenous levels CO can act as a toxin and cause arrhythmogenesis and death. While previous studies have shown carbon monoxide (CO) inhibits Kir 2.x channels in cardiomyocytes, we sought to see whether we could reproduce this result in the heterologous Xenopus system and aim to identify CO-sensitive residues as we did for hydrogen sulfide.

When CORM2 (100 uM), a Rubidium-based CO donor, was applied directly to whole oocytes expressing Kir channels, we observed ~40% steady-state inhibition in Kir2.3 channel current and no change in current in the Kir2.1 channel (Fig. 16), characteristic of the ability of hydrogen sulfide's ability to inhibit Kir2.3 channel and its inability to inhibit the Kir2.1 channel that displays stronger channel- PIP_2 interactions. CO-mediated inhibition of about 55% was recapitulated in Kir3.1* currents. However, the inhibitory effect of CORM2 on Kir2.3 was abolished when the cysteine residue (C28) analogous to Kir3.2* (C53), near the direct channel interaction site with PIP_2, was mutated to alanine (Fig 17). In addition, CO (100uM CORM2) was able to inhibit the Kir2.3 channel when a different cysteine residue (C160) was mutated to alanine, indicating that C28 may specifically confer CO-sensitivity to Kir2.3 channels.

CORM2 was also able to inhibit Kir2.3 channels expressed in macropatch preparations, devoid of cytoplasmic constituents in a dose-dependent manner whether the current was being

evoked submaximally by diC8 (Fig. 18A) or maximally by long-chain PIP_2. (Fig 18B). Analogous to the inhibition by hydrogen sulfide of macropatches expressing Kir2.3, CORM2 increased the pEC50 of PIP2 from 25 μM to 45 μM and reduced the efficacy by 65%. Combined with the TEVC data, we present preliminary evidence which shows that CO acts on specific residues in K channels to modulate channel-PIP_2 interactions and thus channel activity. The cysteine residues on Kir channels may serve as a hub for competing gasotransmitters, hydrogen sulfide, carbon monoxide, as well as nitric oxide (not tested) in physiological or pathophysiological conditions.

Figure 16. Carbon Monoxide (CO) Inhibition of Kir2.3 Channels is PIP_2-dependent. Direct application of Kir2.3 channels with 100 uM CORM2 inhibits channel activity. A. CORM2 inhibits Kir2.3 (IRK3) channel and Kir3.1* channel activities but has no effect on Kir2.1 (IRK1) channel activity. * indicates comparison to the untreated group. Triple symbols indicate p < 0.001.

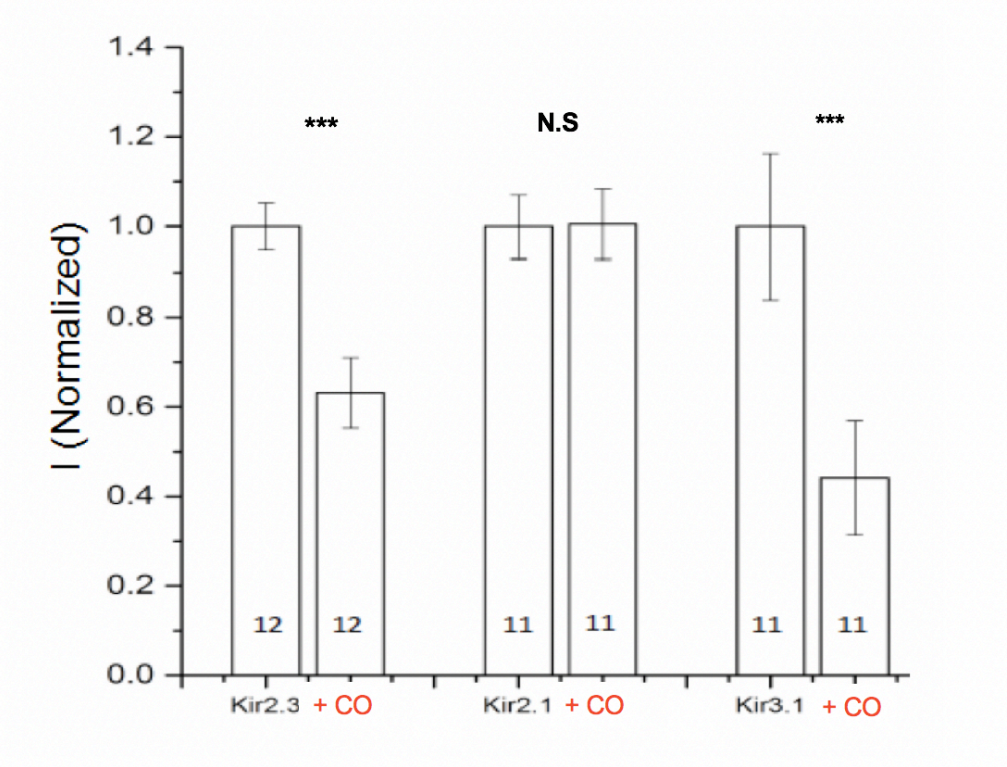


Figure 17. CO Inhibition of Kir2.3 Channels depends on Cysteine 28 (and not Cys 170). Kir2.3 (C28A) activity is entirely insensitive to CORM2. CORM2 application is unable to inhibit Kir2.3 mutant. Mutation of single cysteine residue at position 170 does nothing to alter Kir2.3 sensitivity to CO inhibition. * indicates comparison to untreated group. Triple symbols indicate $p < 0.001$.

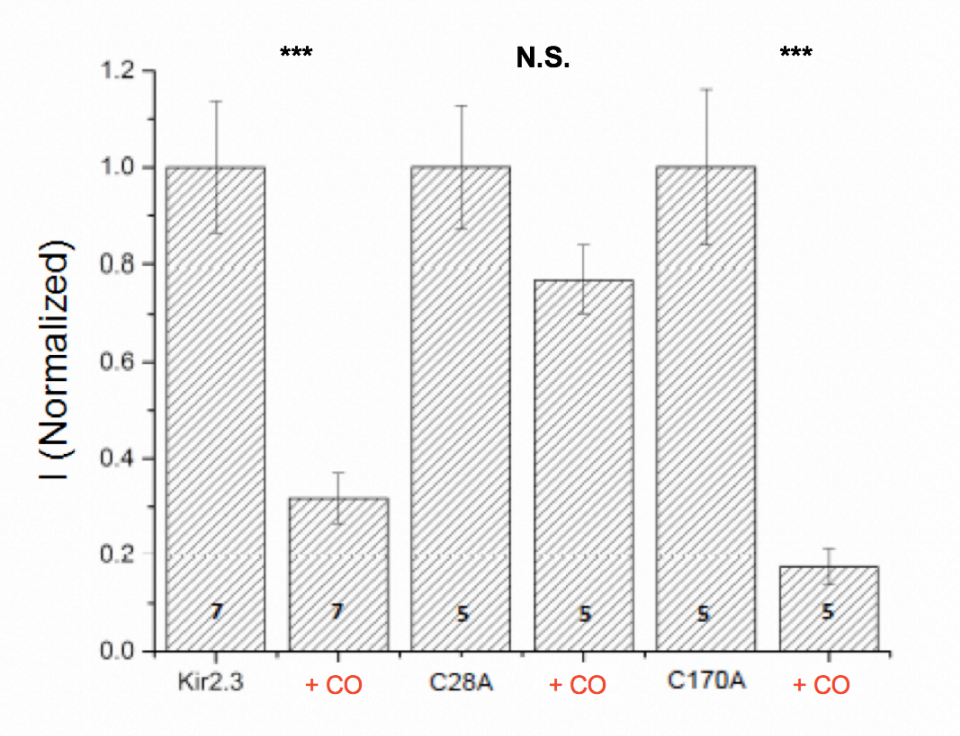
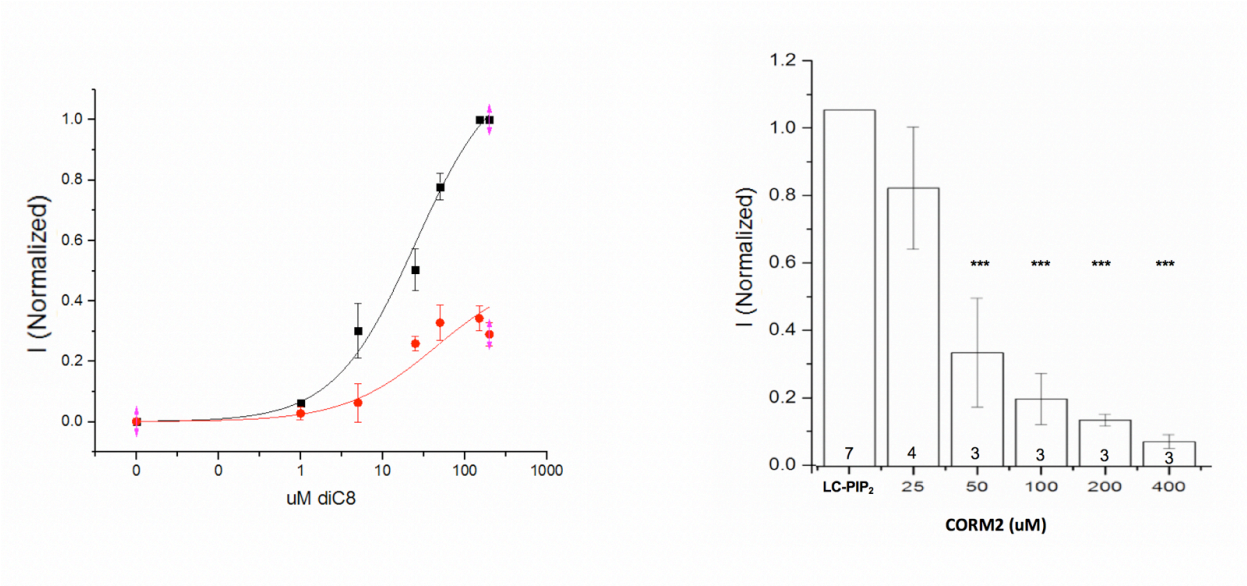


Figure 18. CO Inhibits Kir2.3 Channels in Macropatches in a Dose-Dependent Manner. A. Carbon monoxide (100 µM CORM2) reduces the efficacy and potency of Kir2.3 channel activation by soluble PIP_2 (diC8). B. CO also inhibits Kir2.3 channel activity in macropatches maximally activated by LC-PIP_2 (full-length PIP_2). Direct administration of varying CORM2 concentrations to the cytoplasmic surface of inside-out patches expressing Kir2.3 channels led to concentration-dependent inhibition of Kir2.3 channel activity when they are activated by full length PIP_2.



Chapter 5. Discussion

The "dual functional effect" exerted by hydrogen sulfide is exemplified by neuronal versus cardiovascular cells that are deprived of oxygen. H_2S mediates ischemic damage pursuant to stroke in neuronal tissue [85], whereas it serves as a powerful cardioprotective agent upon comparable conditions. One categorical correlation that emerged in the studies highlighting this 'dual physiological effect' by the gaseous mediator is that while H_2S depolarizes cerebral components [86-90], it hyperpolarizes cardiomyocytes [75, 84]. In other words, H_2S increases the excitability of cerebral tissue, worsening seizure-like symptoms and becoming more susceptible to ischemic insult [85, 89]. In contrast, it depresses the excitability of the heart, in which H_2S is cardioprotective in ischemia and reperfusion (I/R) injury models when administered either through a pre-I/R [16, 76, 77] or post-I/R [78] treatment. The link between the effect of H_2S on tissue excitability and the clinical phenotype is especially evident when the blocking of a single ion channel, $K_{ATP,}$ by glibenclamide, abrogated the cardioprotective effects H_2S had on the I/R injury models [77, 78]. Thus, subsequent efforts have been made to identify key ion channels that contribute to the depolarizing effect of H_2S on neuronal cells as K_{ATP} mediates hyperpolarization in the cardiovascular system and have been inconclusive in identifying the specific ion channels affected in specific neuronal tissues [86-90]. Relying on ion channel blockers with limited specificity has made it difficult to reliably pin the effect of H_2S on observed depolarizations in neurons to specific ion channels. For example, a dose of blockers applied, like TEA that is a non-specific K^+ channel blocker, would barely block most K^+ channels in native tissues [100]. Notably, several members of the Kir family of K^+ channels (Kir2.x and Kir3.x) like other K^+ channels that are not readily blocked by the concentration of agents used in these experiments, are intriguing potential targets of H_2S as they are differentially

expressed in neuronal and cardiac tissues, where they establish the resting membrane potential and modulate their excitability [81].

Here we show for the first time that NaHS inhibits Kir2.x and Kir3.x channels expressed heterologously in *Xenopus* oocytes (Fig. 8), while it activates the closely related cardiac and pancreatic subunit of the K_{ATP} channel subtype, Kir6.2 (confirming previous experiments on the effect H_2S has on other Kir6.x subtypes). The significant inhibition of Kir2.x and Kir3.x channels is surprising given their homology to Kir6.x and is consistent with the depolarizations observed in NaHS-treated native cerebral components. Furthermore, we have demonstrated that NaHS administration can directly sulfhydrate purified Kir3.2 channels (Fig. 8C) *in vitro*, via the TAG Switch Assay (TSA). As with other known modulators of Kir channel activity, we have demonstrated that the effect of H_2S on Kir channels proceeds by altering the strength of channel-PIP_2 interactions. Bolstering channel-PIP_2 interactions (Fig. 10A, 10C, 10D) protected Kir channels from H_2S effects, whereas Kir channels became more susceptible to H_2S when channel-PIP_2 interactions were weakened (Fig. 10A, 10B). We also show here, that the inhibitory effect of H_2S on Kir3.2* channel is mediated by two of four cytoplasmic cysteine residues, C65 and C321 (but not C190 and C221) in each of four channel subunits that form tetrameric Kir3.2 channels. The substitution of all four cytoplasmic cysteines abolished the inhibitory effect of H_2S, without altering the strength of channel-PIP_2 interactions (Fig. 12). The reintroduction of cysteines into positions 65 or 321 in the background of the Kir3.2* Cys-less mutant partially restored H_2S-mediated inhibition, and reintroduction of both cysteines fully restored the extent of H_2S mediated inhibition. Our computational MD simulations experiments that modelled the structural changes upon sulfhydration of Kir3.2 channel provided predictions that are in

agreement with the experimental data. Direct sulfhydration of specific cysteines, C65 and C321 (and not C190) led to increased distances between K64 residue and PIP_2 phosphates (Fig. 14A and Table 1) as well as changes in the G-loop gate favoring the closed conformation (Fig. 14C-D) providing mechanistic insight into the inhibitory effect of H_2S.

While previous experiments have applied micromolar (5-200 μM) concentrations of NaHS, within the physiological range of reported hydrogen sulfide in mammals [85], we administered a 10-fold higher concentration of NaHS (2,000 μM) to elicit a significant response in *Xenopus* oocytes. We attribute this extended treatment (for 100 minutes) and increased NaHS concentration requirement to the expansive size of *Xenopus* oocyte, relative to mammalian cells exposed to NaHS, as well as the stockpiling of beta-globin in these cells, that could serve as a major buffer for hydrogen sulfide [101]. It is noteworthy that this stringent NaHS administration led to channel-specific inhibitory effects, as it was unable to affect Kir2.1 channel activity as well as the Kir3.2* (I234L) mutant, two channels displaying higher apparent affinities to PIP_2, whereas it activated (rather than inhibited) Kir6.2 channels. Still, in order to ensure we are not observing toxic effects of NaHS on Kir channels, we demonstrated that the inhibitory effect of NaHS on Kir3.2* channels could be mimicked by facilitating endogenous production of hydrogen sulfide through the co-expression in *Xenopus* oocytes of cystathionine γ-lyase (CSE), a key producer of endogenous H_2S in native cardiovascular and specific neuronal tissues. As with oocytes administered NaHS, the Kir3.2*(I234L) mutant, with increased apparent channel-PIP_2 affinity, was refractory inhibition when co-expressed with CSE, and co-incubation with PAG, an inhibitor of CSE, abolished the inhibition of Kir3.2* channels. Additionally, we employed NaHS in the micromolar range of concentrations directly to the cytoplasmic side of *Xenopus* inside-out

patches expressing Kir 2.3 channels in inside-out macropatches, separating the membrane-delimited elements from the rest of the cellular cytoplasm. As expected, Kir2.3 channel activity was greatly inhibited (Fig. 10A) by much lower concentrations of NaHS in a dose-dependent manner (IC_{50} ~83 μM), and channel activity was maximally inhibited by ~64%, similar to the inhibition measured in whole oocytes incubated with stringent levels of NaHS (Fig. 8D). Interestingly, maximally activating patches with Kir3.2* with long chain PIP_2 (2 μM) exhibited lesser NaHS-mediated inhibition (~37% maximal inhibition) compared to when Kir2.3 channels are activated by a submaximal concentration of PIP_2 (25 μM diC8 PIP_2, Fig. 10A), consistent with the diminished NaHS inhibition when channel-PIP_2 interactions were strengthened in the whole oocyte experiments (Fig. 9). Also, PIP_2 efficacy and potency were weakened by NaHS treatment (Fig. 10C) indicated by the ~29% reduction in maximal activity and a rightward shift of the diC8 PIP_2 dose-response curve respectively following NaHS treatment. These findings are consistent with the MD computational simulation results, in which conformational changes are induced by sulfhydration of cysteine residues, leading to weakened channel-PIP_2 interactions and the closing of the G-Loop gate (Fig. 14). Interestingly, our computational predictions are also in agreement with the activation of Kir 6.2 by H_2S (Fig. 8E), showing sulfhydration of C42 (works in a way opposite to modification of cysteines in the Kir3.2 model) in a homology model of Kir6.2 (based on the Kir3.2 structure), leads to strengthening of channel-PIP_2 interactions and opening of the G-Loop gate (Fig. 15).

The mechanisms underlying differential regulation of Kir6.x channels from that of Kir3.x channels need to be further explored. Despite sharing remarkable homology, hydrogen sulfide has an activating effect on Kir 6.x channels opposite of its inhibitory effect on Kir 2.x and Kir3.x channels, revealed by the results in this thesis. Whether hydrogen sulfide's activating effects on

Kir 6.x is solely mediated through C42 needs to evaluated by similar cysteine-mutation experiments done with Kir 3.2 channels. In addition, the direct sulfhydration of Kir 6.x channels requires testing by TAG-switch assay and mass spectrometry as there are existing conflicting modified Biotin switch assays that potentially complicate whether the Kir6.x channels or auxiliary SUR subunits are directly sulfhydrated.

We demonstrate the effect of H_2S on Kir2.x and Kir3.x is inhibitory, in the opposite direction of the previously characterized Kir6.x channel activation despite their homology. Their inhibition by H_2S could be a critical factor in the NaHS-mediated depolarizations observed in native tissue compartments like in neurons, as Kir2.x and Kir3.x inhibition would have a depolarizing influence on specific tissue types that express these subtypes, making them more excitable. Whereas activation of Kir channels (Kir6.), such as in cardiomyocytes or colonic smooth muscle cells [102] would have the opposite hyperpolarizing influence on specific cell types that express this Kir subtype robustly, making them less excitable. Our findings may provide a potential explanation for the depolarization of certain specific cells, while they do not rule out a role for other affected ion channels. Future studies evaluating the collective effect of H_2S on specific native brain tissues will need to at least address the differential expression of Kir channels [103]. One explanation as to why H_2S raises the excitability of specific tissues may be because its depolarizing influence via inhibition of Kir2.x and Kir3.x channels is simply greater than its opposing influence on Kir6.x channels (whereas the hyperpolarizing influence of H_2S dominates in specific tissue cell types, like native cardiomyocytes and smooth muscle cells). Here, we also show that the inhibitory effect of H_2S is PIP_2-dependent, in which increasing the strength of channel-PIP_2 interactions protects the Kir2.x and Kir3.x channels from H_2S inhibition

and weakening them makes them more susceptible to H_2S inhibition. Our work identifies new physiological targets of H_2S and offers mechanistic insights into the inhibition of Kir channels by H_2S.

Chapter 6. Future Directions

The major physiological undercurrent of this thesis work that the varied tissue-specific changes in membrane potential (depolarization or hyperpolarization) in response to hydrogen sulfide may be, to a certain extent, explained by the differential expression of Kir channels in various tissues requires further examination. More specifically, specific cells (like neurons) with greater hydrogen sulfide effect on Kir2.x/3.x channels relative to that on Kir6.x channels would elicit a net depolarized change whereas cells with greater hydrogen sulfide effect on Kir6.x channels would yield a net hyperpolarizing effect. Thus, hydrogen sulfide may exert disparate depolarizing or hyperpolarizing influence on the tissue cell type depending on its competing inhibitory influence between Kir2.x/Kir3.x channels and Kir6.x channels. The results in this thesis clearly demonstrate that the sulfhydration of cytoplasmic cysteine residues in the Kir channel alters gating and activation by the phospholipid PIP_2 in a heterologous *Xenopus laevis* system. Future experiments need to address the actions of hydrogen sulfide on native mammalian cells such as neurons that express a differential mixed population of Kir channels (Kir2.x/Kir3.x, Kir 6.x channels, as well as other Na^+, Ca^{2+}, and Cl^- channels) and determine whether the results in the heterologous system can explain the net effect on native cells. Previous experiments have shown that hydrogen sulfide has a depolarizing effect on neurons [86-89], but they have been unable to determine which ion channels are eliciting the hydrogen sulfide-mediated depolarization. The common strategy in these endeavors has been to co-apply selective ion

channel blockers simultaneously with hydrogen sulfide to see which channel blocker reverses the depolarizing effect on neurons. Given the results in this thesis, future experiments ought to use more selective blockers of Kir Channels such as Tertiapin Q (specific blocker of Kir1.1, Kir3.1/3.4, and Kir3.1/Kir3.2 channels) simultaneously with hydrogen sulfide rather than TEA, employed by previous experiments, which at the reported range of concentrations is unable to block Kir channel currents. Also, previous experiments assaying the effects of hydrogen sulfide on cardiomyocytes often demonstrate the hyperpolarizing effects based on narrow concentration of hydrogen sulfide and dismiss any reversal of the hyperpolarizing effect without adequate explanation. Future experiments need to apply increasing concentrations of NaHS on native cardiac cells to observe whether differential pharmacological effects occur, such as the NaHS being able to influence greater population of Kir channels other than Kir6.1.

While this thesis work provides invaluable mechanistic explanation as to how hydrogen sulfide inhibits Kir2.x and Kir3.x channels, single-channel experiments could further elucidate whether the hydrogen sulfide 1. removes functional channels from the population, 2. reduces the unitary conductance of channels, and/or 3. reduces the mean open probability of the channel. Previous single channel recording studies have already shown that NaHS affects Kir6.x channel opening, rather than the number of functional Kir6.x channels at the membrane or unitary conductance.

Some other ambiguities still persist in the mechanism underlying Kir channel inhibition by hydrogen sulfide. For example, it is not exactly clear how strengthening channel-PIP_2 interactions protects Kir channels from inhibition by hydrogen sulfide, and how weakening channel-PIP_2 interactions intensifies the hydrogen sulfide inhibitory effect. One explanation is

that channel-PIP_2 interactions simply protect specific cysteine residues from sulfhydration by hydrogen sulfide, thereby preventing the hydrogen sulfide effect. Another explanation is that the cysteine residues are not protected, and hydrogen sulfide is able to sulfhydrate the specific cysteine residues readily and exert an inhibitory effect on the channel in opposition to the net stimulatory influence by PIP_2. If hydrogen sulfide were to win out in this "tug of war" model and overcome the channel-PIP_2 interactions, it would also be able to exert a net inhibitory effect whereas no net effect would occur if channel-PIP_2 interactions are able to overpower the inhibitory influence placed by sulfhydrated cysteine residues. The distinction between these two simplified models may be tested by employing the TAG Assay and observing whether channel sulfhydration levels are affected by co-administration of PIP_2 (although, the TAG Assay method in this thesis removes the channel from the lipid bilayer environment).

Interestingly, NaHS not only weakens channel-PIP_2 interactions by increasing the diC8 EC_{50} (Fig. 10B) but it also reduces the efficacy of the channel so that additional PIP_2 is unable to maximally activate the patch containing the channels modified by NaHS. The macropatch set up also gives us the opportunity to conduct future experiments that examine whether NaHS has a channel state dependent effect, whether the open or closed state of the channel affects the extent of NaHS inhibition. It would not be surprising if future experiments revealed that activated channels have more resilience to NaHS inhibition, given there would be more PIP_2 within the vicinity of the channel. The converse would be true given, there is less channel activation when there is less PIP_2 in the vicinity.

The TAG assay (Fig. 8B) results in this thesis is encouraging but not sufficient in providing evidence that Kir3.2 channel is directly sulfhydrated by exogenous NaHS. Additional

TAG assay experiments with controls, such as purified channel protein (not exposed to NaHS) and increasing concentrations of NaHS, and NaHS exposure of channel proteins lacking specific cysteine residues would reveal whether 1) purified channel is endogenously sulfhydrated (and to what extent), 2) increasing NaHS exposure alters the extent of channel sulfhydration, and 3) specific cysteine residues are differentially sulfhydrated. For example, if purified Kir3.2 channel lacking cysteine residues does not get pulled down by streptavidin would inspire greater confidence in the TAG assay. Additionally, the field would benefit greatly if mass spectrometry experiments would provide another independent approach to show sulfhydration by hydrogen sulfide on the specific cysteine residues as well as other post-translational modifications that are not limited to the specific cysteine residues. Post-translational coverage by mass spectrometry would also reveal other potential modifications on the cysteine residues (as well as all residues on the protein) and merits overcoming the challenge that lies in optimizing mass spectrometry conditions to allow for better coverage of modified Kir residues.

Another technical issue in electrophysiological experiments using NaHS is that hydrogen sulfide rapidly evaporates into the open atmosphere, requiring the immediate use of NaHS solutions just prior to experiments. Previous experiments have implied that nearly 75% of hydrogen sulfide can dissolve out of aqueous solution within 30 minutes, casting some uncertainty to how representative the actual hydrogen sulfide concentration values used in the TEVC and macropatch experiments. Future experiments could utilize another hydrogen sulfide donor that releases hydrogen sulfide less rapidly than NaHS to prevent the rapid loss of hydrogen sulfide in open experimental solutions. In addition, future experiments can be performed in more closed experimental environments to prevent diffusion of hydrogen sulfide at the reservoir.

In addition, we have preliminary evidence (data not shown) that increasing PIP_2 levels diminishes the activating effect of hydrogen sulfide on Kir6.x channels, which is consistent with our results that increasing channel-PIP_2 interactions reduces the inhibitory hydrogen sulfide effect in Kir2.x and Kir3.x channels. The mechanisms underlying how hydrogen sulfide differentially regulates Kir2.x/Kir3.x channels and Kir6.x channels requires further exploration, given that the Kir channels, despite belonging to the same family, have diametrically opposite responses to hydrogen sulfide. One putative reason for the different responses may be that hydrogen sulfide may relieve Kir6.x channels from tonic inhibition by ATP (which does not affect other Kir channels). Expressing Kir6.x channels in macropatches and exposing them to different rage of NaHS and ATP to the cytoplasmic side of the patch would clearly show whether NaHS affects channel inhibition by ATP. Extensive future experiments that swap structural motifs (or amino acids) distinct between Kir2.x/3.x and Kir6.x channels may reveal key structural determinants that elicit inhibitory or stimulatory response to hydrogen sulfide.

Lastly, the specific cysteine residues that play a critical role in NaHS regulation may also be subjected to differential regulation by other gasotransmitters like carbon monoxide (CO) and nitric oxide (NO), that are ubiquitous players under physiological and pathophysiological circumstances. Already, experiments on Kir channels with CORM2 have revealed that one of the cysteines involved in hydrogen sulfide regulation may also be involved in CO mediated inhibition. Future experiments will need to address the reversibility of the hydrogen sulfide effect, as well as how carbon monoxide (briefly discussed in this thesis) or nitric oxide (via nitrosylation, not explored in this thesis) may compete with or add to hydrogen sulfide inhibition on Kir channels and how the extent of their regulation may also be dependent on channel PIP_2 interactions.

Chapter 7. Literature Cited

1. Wang, R., *Physiological implications of hydrogen sulfide: a whiff exploration that blossomed.* Physiol Rev, 2012. **92**(2): p. 791-896.

2. Haahtela, T., et al., *The South Karelia Air Pollution Study: acute health effects of malodorous sulfur air pollutants released by a pulp mill.* Am J Public Health, 1992. **82**(4): p. 603-5.

3. Snyder, J.W., et al., *Occupational fatality and persistent neurological sequelae after mass exposure to hydrogen sulfide.* Am J Emerg Med, 1995. **13**(2): p. 199-203.

4. Wang, R., *Toxic gas, lifesaver.* Sci Am, 2010. **302**(3): p. 66-71.

5. Goodwin, L.R., et al., *Determination of sulfide in brain tissue by gas dialysis/ion chromatography: postmortem studies and two case reports.* J Anal Toxicol, 1989. **13**(2): p. 105-9.

6. Warenycia, M.W., et al., *Acute hydrogen sulfide poisoning. Demonstration of selective uptake of sulfide by the brainstem by measurement of brain sulfide levels.* Biochem Pharmacol, 1989. **38**(6): p. 973-81.

7. Paul, B.D. and S.H. Snyder, *H2S: A Novel Gasotransmitter that Signals by Sulfhydration.* Trends Biochem Sci, 2015. **40**(11): p. 687-700.

8. Ogasawara, Y., et al., *Determination of bound sulfur in serum by gas dialysis/high-performance liquid chromatography.* Anal Biochem, 1993. **215**(1): p. 73-81.

9. Ogasawara, Y., S. Isoda, and S. Tanabe, *Tissue and subcellular distribution of bound and acid-labile sulfur, and the enzymic capacity for sulfide production in the rat.* Biol Pharm Bull, 1994. **17**(12): p. 1535-42.

10. Toohey, J.I., *Sulphane sulphur in biological systems: a possible regulatory role.* Biochem J, 1989. **264**(3): p. 625-32.

11. Ishigami, M., et al., *A source of hydrogen sulfide and a mechanism of its release in the brain.* Antioxid Redox Signal, 2009. **11**(2): p. 205-14.

12. Iciek, M. and L. Wlodek, *Biosynthesis and biological properties of compounds containing highly reactive, reduced sulfane sulfur.* Pol J Pharmacol, 2001. **53**(3): p. 215-25.

13. Salloum, F.N., *Hydrogen sulfide and cardioprotection--Mechanistic insights and clinical translatability.* Pharmacol Ther, 2015. **152**: p. 11-7.

14. Paul, B.D. and S.H. Snyder, *H(2)S signalling through protein sulfhydration and beyond.* Nat Rev Mol Cell Biol, 2012. **13**(8): p. 499-507.

15. Yang, G., et al., *H2S as a physiologic vasorelaxant: hypertension in mice with deletion of cystathionine gamma-lyase.* Science, 2008. **322**(5901): p. 587-90.

16. Elrod, J.W., et al., *Hydrogen sulfide attenuates myocardial ischemia-reperfusion injury by preservation of mitochondrial function.* Proc Natl Acad Sci U S A, 2007. **104**(39): p. 15560-5.

17. Zanardo, R.C., et al., *Hydrogen sulfide is an endogenous modulator of leukocyte-mediated inflammation.* FASEB J, 2006. **20**(12): p. 2118-20.

18. Wang, R., *Is H2S a stinky remedy for atherosclerosis?* Arterioscler Thromb Vasc Biol, 2009. **29**(2): p. 156-7.

19. Wang, Y., et al., *Role of hydrogen sulfide in the development of atherosclerotic lesions in apolipoprotein E knockout mice.* Arterioscler Thromb Vasc Biol, 2009. **29**(2): p. 173-9.

20. Wu, L., et al., *Pancreatic islet overproduction of H2S and suppressed insulin release in Zucker diabetic rats.* Lab Invest, 2009. **89**(1): p. 59-67.

21. Wu, R., et al., *[Plasma level of endogenous hydrogen sulfide in patients with acute asthma].* Beijing Da Xue Xue Bao, 2008. **40**(5): p. 505-8.

22. Qiu, X., et al., *Role of Hydrogen Sulfide in the Physiology of Penile Erection.* Journal of andrology, 2012. **33**(4): p. 529-535.

23. Braunstein, A.E., E.V. Goryachenkova, and N.D. Lac, *Reactions catalysed by serine sulfhydrase from chicken liver.* Biochim Biophys Acta, 1969. **171**(2): p. 366-8.

24. Banerjee, R. and C.G. Zou, *Redox regulation and reaction mechanism of human cystathionine-beta-synthase: a PLP-dependent hemesensor protein.* Arch Biochem Biophys, 2005. **433**(1): p. 144-56.

25. Yamanishi, M., et al., *Structural insights into pathogenic mutations in heme-dependent cystathionine-beta-synthase.* J Inorg Biochem, 2006. **100**(12): p. 1988-95.

26. Cantoni, G.L., *THE NATURE OF THE ACTIVE METHYL DONOR FORMED ENZYMATICALLY FROM L-METHIONINE AND ADENOSINETRIPHOSPHATE1,2.* Journal of the American Chemical Society, 1952. **74**(11): p. 2942-2943.

27. Lee, M., et al., *Astrocytes produce the antiinflammatory and neuroprotective agent hydrogen sulfide.* Neurobiol Aging, 2009. **30**(10): p. 1523-34.

28. Abe, K. and H. Kimura, *The possible role of hydrogen sulfide as an endogenous neuromodulator.* J Neurosci, 1996. **16**(3): p. 1066-71.

29. Watanabe, M., et al., *Mice deficient in cystathionine beta-synthase: animal models for mild and severe homocyst(e)inemia.* Proc Natl Acad Sci U S A, 1995. **92**(5): p. 1585-9.

30. Nagahara, N., et al., *Tissue and subcellular distribution of mercaptopyruvate sulfurtransferase in the rat: confocal laser fluorescence and immunoelectron microscopic studies combined with biochemical analysis.* Histochemistry and Cell Biology, 1998. **110**(3): p. 243-250.

31. Shibuya, N., et al., *3-Mercaptopyruvate sulfurtransferase produces hydrogen sulfide and bound sulfane sulfur in the brain.* Antioxid Redox Signal, 2009. **11**(4): p. 703-14.

32. Kuo, S.M., T.C. Lea, and M.H. Stipanuk, *Developmental pattern, tissue distribution, and subcellular distribution of cysteine: alpha-ketoglutarate aminotransferase and 3-mercaptopyruvate sulfurtransferase activities in the rat.* Biol Neonate, 1983. **43**(1-2): p. 23-32.

33. Crawhall, J.C., *A review of the clinical presentation and laboratory findings in two uncommon hereditary disorders of sulfur amino acid metabolism, beta-mercaptolactate cysteine disulfideuria and sulfite oxidase deficiency.* Clin Biochem, 1985. **18**(3): p. 139-42.

34. Mustafa, A.K., et al., *H2S signals through protein S-sulfhydration.* Sci Signal, 2009. **2**(96): p. ra72.

35. Hara, M.R., et al., *S-nitrosylated GAPDH initiates apoptotic cell death by nuclear translocation following Siah1 binding.* Nat Cell Biol, 2005. **7**(7): p. 665-74.

36. Benhar, M., et al., *Regulated Protein Denitrosylation by Cytosolic and Mitochondrial Thioredoxins.* Science (New York, N.Y.), 2008. **320**(5879): p. 1050-1054.

37. Zhang, D., et al., *Detection of protein S-sulfhydration by a tag-switch technique.* Angew Chem Int Ed Engl, 2014. **53**(2): p. 575-81.

38. Hongfang, J., et al., *Effects of hydrogen sulfide on hypoxic pulmonary vascular structural remodeling.* Life Sci, 2006. **78**(12): p. 1299-309.

39. Hyspler, R., et al., *A simple, optimized method for the determination of sulphide in whole blood by GC-mS as a marker of bowel fermentation processes.* J Chromatogr B Analyt Technol Biomed Life Sci, 2002. **770**(1-2): p. 255-9.

40. Richardson, C.J., E.A. Magee, and J.H. Cummings, *A new method for the determination of sulphide in gastrointestinal contents and whole blood by microdistillation and ion chromatography.* Clin Chim Acta, 2000. **293**(1-2): p. 115-25.

41. Zhao, W., et al., *The vasorelaxant effect of H(2)S as a novel endogenous gaseous K(ATP) channel opener.* EMBO J, 2001. **20**(21): p. 6008-16.

42. Chen, Y.H., et al., *Endogenous hydrogen sulfide in patients with COPD.* Chest, 2005. **128**(5): p. 3205-11.

43. Hosoki, R., N. Matsuki, and H. Kimura, *The possible role of hydrogen sulfide as an endogenous smooth muscle relaxant in synergy with nitric oxide.* Biochem Biophys Res Commun, 1997. **237**(3): p. 527-31.

44. Hu, L.F., et al., *Hydrogen sulfide inhibits rotenone-induced apoptosis via preservation of mitochondrial function.* Mol Pharmacol, 2009. **75**(1): p. 27-34.

45. Doeller, J.E., et al., *Polarographic measurement of hydrogen sulfide production and consumption by mammalian tissues.* Anal Biochem, 2005. **341**(1): p. 40-51.

46. Furne, J., A. Saeed, and M.D. Levitt, *Whole tissue hydrogen sulfide concentrations are orders of magnitude lower than presently accepted values.* Am J Physiol Regul Integr Comp Physiol, 2008. **295**(5): p. R1479-85.

47. Flavin, M. and C. Slaughter, *Enzymatic synthesis of homocysteine or methionine directly from O-succinyl-homoserine.* Biochim Biophys Acta, 1967. **132**(2): p. 400-5.

48. Jhee, K.H. and W.D. Kruger, *The role of cystathionine beta-synthase in homocysteine metabolism.* Antioxid Redox Signal, 2005. **7**(5-6): p. 813-22.

49. Gainey, D., S. Short, and K.L. McCoy, *Intracellular location of cysteine transport activity correlates with productive processing of antigen disulfide.* Journal of Cellular Physiology, 1996. **168**(2): p. 248-254.

50. Elsey, D.J., R.C. Fowkes, and G.F. Baxter, *L-cysteine stimulates hydrogen sulfide synthesis in myocardium associated with attenuation of ischemia-reperfusion injury.* J Cardiovasc Pharmacol Ther, 2010. **15**(1): p. 53-9.

51. Mani, S., G. Yang, and R. Wang, *A critical life-supporting role for cystathionine gamma-lyase in the absence of dietary cysteine supply.* Free Radic Biol Med, 2011. **50**(10): p. 1280-7.

52. Ishii, I., et al., *Cystathionine gamma-Lyase-deficient mice require dietary cysteine to protect against acute lethal myopathy and oxidative injury.* J Biol Chem, 2010. **285**(34): p. 26358-68.

53. Zhang, M., et al., *Selective phosphorylation modulates the PIP2 sensitivity of the CaM–SK channel complex.* Nat Chem Biol, 2014. **10**(9): p. 753-759.

54. Adney, S.K., et al., *A Critical Gating Switch at a Modulatory Site in Neuronal Kir3 Channels.* J Neurosci, 2015. **35**(42): p. 14397-405.

55. Fan, Z. and J.C. Makielski, *Anionic phospholipids activate ATP-sensitive potassium channels.* J Biol Chem, 1997. **272**(9): p. 5388-95.

56. Hilgemann, D.W. and R. Ball, *Regulation of cardiac Na+,Ca2+ exchange and KATP potassium channels by PIP2.* Science, 1996. **273**(5277): p. 956-9.

57. Sui, J.L., J. Petit-Jacques, and D.E. Logothetis, *Activation of the atrial KACh channel by the betagamma subunits of G proteins or intracellular Na+ ions depends on the presence of phosphatidylinositol phosphates.* Proc Natl Acad Sci U S A, 1998. **95**(3): p. 1307-12.

58. Tucker, S.J. and T. Baukrowitz, *How highly charged anionic lipids bind and regulate ion channels.* J Gen Physiol, 2008. **131**(5): p. 431-8.

59. Hilgemann, D.W., *Local PIP(2) signals: when, where, and how?* Pflugers Arch, 2007. **455**(1): p. 55-67.

60. McLaughlin, S., et al., *PIP(2) and proteins: interactions, organization, and information flow.* Annu Rev Biophys Biomol Struct, 2002. **31**: p. 151-75.

61. Xu, C., J. Watras, and L.M. Loew, *Kinetic analysis of receptor-activated phosphoinositide turnover.* J Cell Biol, 2003. **161**(4): p. 779-91.

62. Gamper, N. and M.S. Shapiro, *Regulation of ion transport proteins by membrane phosphoinositides.* Nat Rev Neurosci, 2007. **8**(12): p. 921-34.

63. Lehninger, A.L., D.L. Nelson, and M.M. Cox, *Lehninger principles of biochemistry*. 5th ed. 2008, New York: W.H. Freeman. 1 v. (various pagings).

64. Suh, B.C. and B. Hille, *PIP2 is a necessary cofactor for ion channel function: how and why?* Annu Rev Biophys, 2008. **37**: p. 175-95.

65. Logothetis, D.E., et al., *Phosphoinositide-mediated gating of inwardly rectifying K(+) channels.* Pflugers Arch, 2007. **455**(1): p. 83-95.

66. Rohacs, T., et al., *Distinct specificities of inwardly rectifying K(+) channels for phosphoinositides.* J Biol Chem, 1999. **274**(51): p. 36065-72.

67. Rohacs, T., et al., *Specificity of activation by phosphoinositides determines lipid regulation of Kir channels.* Proc Natl Acad Sci U S A, 2003. **100**(2): p. 745-50.

68. Zhang, H., et al., *Activation of inwardly rectifying K+ channels by distinct PtdIns(4,5)P2 interactions.* Nat Cell Biol, 1999. **1**(3): p. 183-8.

69. Du, X., et al., *Characteristic interactions with phosphatidylinositol 4,5-bisphosphate determine regulation of kir channels by diverse modulators.* J Biol Chem, 2004. **279**(36): p. 37271-81.

70. Rodriguez-Menchaca, A.A., et al., *PIP2 controls voltage-sensor movement and pore opening of Kv channels through the S4-S5 linker.* Proc Natl Acad Sci U S A, 2012. **109**(36): p. E2399-408.

71. An, H.-L., et al., *The Cytosolic GH Loop Regulates the Phosphatidylinositol 4,5-Bisphosphate-induced Gating Kinetics of Kir2 Channels.* Journal of Biological Chemistry, 2012. **287**(50): p. 42278-42287.

72. Fuster, V. and B.B. Kelly, in *Promoting Cardiovascular Health in the Developing World: A Critical Challenge to Achieve Global Health*. 2010: Washington (DC).

73. Kimura, H., *The physiological role of hydrogen sulfide and beyond.* Nitric Oxide, 2014. **41**: p. 4-10.

74. Krishnan, N., et al., *H2S-Induced sulfhydration of the phosphatase PTP1B and its role in the endoplasmic reticulum stress response.* Sci Signal, 2011. **4**(203): p. ra86.

75. Mustafa, A.K., et al., *Hydrogen sulfide as endothelium-derived hyperpolarizing factor sulfhydrates potassium channels.* Circ Res, 2011. **109**(11): p. 1259-68.

76. Bian, J.S., et al., *Role of hydrogen sulfide in the cardioprotection caused by ischemic preconditioning in the rat heart and cardiac myocytes.* J Pharmacol Exp Ther, 2006. **316**(2): p. 670-8.

77. Johansen, D., K. Ytrehus, and G.F. Baxter, *Exogenous hydrogen sulfide (H2S) protects against regional myocardial ischemia-reperfusion injury--Evidence for a role of K ATP channels.* Basic Res Cardiol, 2006. **101**(1): p. 53-60.

78. Zhang, Z., et al., *Hydrogen sulfide contributes to cardioprotection during ischemia-reperfusion injury by opening K ATP channels.* Can J Physiol Pharmacol, 2007. **85**(12): p. 1248-53.

79. Das, A., et al., *Hydrogen sulfide mediates the cardioprotective effects of gene therapy with PKG-Ialpha.* Basic Res Cardiol, 2015. **110**(4): p. 42.

80. Gross, G.J. and R.M. Fryer, *Sarcolemmal versus mitochondrial ATP-sensitive K+ channels and myocardial preconditioning.* Circ Res, 1999. **84**(9): p. 973-9.

81. Hibino, H., et al., *Inwardly rectifying potassium channels: their structure, function, and physiological roles.* Physiol Rev, 2010. **90**(1): p. 291-366.

82. Liang, S., et al., *Carbon monoxide inhibits inward rectifier potassium channels in cardiomyocytes.* Nat Commun, 2014. **5**: p. 4676.

83. Yoo, D., et al., *Analysis of cardiovascular responses to the H2S donors Na2S and NaHS in the rat.* Am J Physiol Heart Circ Physiol, 2015. **309**(4): p. H605-14.

84. Wei, H., et al., *Hydrogen sulfide suppresses outward rectifier potassium currents in human pluripotent stem cell-derived cardiomyocytes.* PLoS One, 2012. **7**(11): p. e50641.

85. McCune, C.D., et al., *"Zipped Synthesis" by Cross-Metathesis Provides a Cystathionine beta-Synthase Inhibitor that Attenuates Cellular H2S Levels and Reduces Neuronal Infarction in a Rat Ischemic Stroke Model.* ACS Cent Sci, 2016. **2**(4): p. 242-52.

86. Feng, X., et al., *Hydrogen sulfide increases excitability through suppression of sustained potassium channel currents of rat trigeminal ganglion neurons.* Mol Pain, 2013. **9**: p. 4.

87. Khademullah, C.S. and A.V. Ferguson, *Depolarizing actions of hydrogen sulfide on hypothalamic paraventricular nucleus neurons.* PLoS One, 2013. **8**(5): p. e64495.

88. Kuksis, M. and A.V. Ferguson, *Actions of a hydrogen sulfide donor (NaHS) on transient sodium, persistent sodium, and voltage-gated calcium currents in neurons of the subfornical organ.* J Neurophysiol, 2015. **114**(3): p. 1641-51.

89. Luo, Y., et al., *Aggravation of seizure-like events by hydrogen sulfide: involvement of multiple targets that control neuronal excitability.* CNS Neurosci Ther, 2014. **20**(5): p. 411-9.

90. Austgen, J.R., et al., *Hydrogen sulfide augments synaptic neurotransmission in the nucleus of the solitary tract.* J Neurophysiol, 2011. **106**(4): p. 1822-32.

91. Logothetis, D.E., et al., *Unifying Mechanism of Controlling Kir3 Channel Activity by G Proteins and Phosphoinositides.* Int Rev Neurobiol, 2015. **123**: p. 1-26.

92. Rohacs, T., et al., *Assaying phosphatidylinositol bisphosphate regulation of potassium channels.* Methods Enzymol, 2002. **345**: p. 71-92.

93. Bodhinathan, K. and P.A. Slesinger, *Molecular mechanism underlying ethanol activation of G-protein-gated inwardly rectifying potassium channels.* Proc Natl Acad Sci U S A, 2013. **110**(45): p. 18309-14.

94. Yi, B.A., et al., *Yeast screen for constitutively active mutant G protein-activated potassium channels.* Neuron, 2001. **29**(3): p. 657-67.

95. Vivaudou, M., et al., *Probing the G-protein regulation of GIRK1 and GIRK4, the two subunits of the KACh channel, using functional homomeric mutants.* J Biol Chem, 1997. **272**(50): p. 31553-60.

96. Tucker, S.J., et al., *Truncation of Kir6.2 produces ATP-sensitive K+ channels in the absence of the sulphonylurea receptor.* Nature, 1997. **387**(6629): p. 179-83.

97. Zerangue, N., et al., *A new ER trafficking signal regulates the subunit stoichiometry of plasma membrane K(ATP) channels.* Neuron, 1999. **22**(3): p. 537-48.

98. Whorton, M.R. and R. MacKinnon, *Crystal structure of the mammalian GIRK2 K+ channel and gating regulation by G proteins, PIP2, and sodium.* Cell, 2011. **147**(1): p. 199-208.

99. Whorton, M.R. and R. MacKinnon, *X-ray structure of the mammalian GIRK2-betagamma G-protein complex.* Nature, 2013. **498**(7453): p. 190-7.

100. Katayama, J., T. Yakushiji, and N. Akaike, *Characterization of the K+ current mediated by 5-HT1A receptor in the acutely dissociated rat dorsal raphe neurons.* Brain Res, 1997. **745**(1-2): p. 283-92.

101. Pietri, R., E. Román-Morales, and J. López-Garriga, *Hydrogen Sulfide and Hemeproteins: Knowledge and Mysteries.* Antioxidants & Redox Signaling, 2011. **15**(2): p. 393-404.

102. Gade, A.R., M. Kang, and H.I. Akbarali, *Hydrogen Sulfide as an Allosteric Modulator of ATP-Sensitive Potassium Channels in Colonic Inflammation.* Molecular Pharmacology, 2013. **83**(1): p. 294-306.

103. Karschin, C., et al., *IRK(1-3) and GIRK(1-4) inwardly rectifying K+ channel mRNAs are differentially expressed in the adult rat brain.* J Neurosci, 1996. **16**(11): p. 3559-70.

Vita

Junghoon Ha was born on June 30, 1981 in Seoul, South Korea. Ha immigrated to the United States on July, 1988. He attended Thomas Jefferson High School for Science and Technology in Alexandria, VA, where he graduated with a Jefferson diploma in 2000. In 2004, he received his BSc. in Biology from University of Virginia in Charlottesville, VA. During his undergraduate studies, he was trained in molecular biology under the mentorship of Dr. Anthony Spano, Research Scientist in the Biology Department. Thereafter, he was trained as a live-cell imaging microscopist under the mentorship of Dr. Kevin Pfister (2004-2007), an Associate Professor of Cell Biology in the Molecular Cell and Developmental Biology Department at the University of Virginia School of Medicine. After he completed his M.S. degree in Physiology in June 2008 in the laboratory of Dr. Diomedes Logothetis at Virginia Commonwealth University, he matriculated in the School of Medicine as a M.D./Ph.D candidate in Aug. 2009. He pursued his Ph.D. thesis in Dr. Logothetis's lab and worked to produce the results that are embodied in this dissertation.